Int J Theor Phys (2010) 49: 1649–1683
DOI 10.1007/s10773-010-0346-x

Semiclassical Loop Quantum Black Hole

Leonardo Modesto

Received: 1 February 2010 / Accepted: 31 March 2010 / Published online: 15 April 2010

Abstract In this paper we improve the semiclassical analysis of loop quantum black hole (LQBH) in the conservative approach of a constant polymeric parameter. In particular we focus our attention on the space-time structure. We introduce a very simple modification of the spherically symmetric Hamiltonian constraint in terms of holonomies. The new quantum constraint reduces to the classical constraint when the polymeric parameter δ goes to zero. Using this modification we obtain a large class of semiclassical solutions parametrized by a generic function $\sigma(\delta)$. We find that only a particular choice of this function reproduces the Schwarzschild black hole solution outside the black hole with the correct asymptotic flat limit. In $r = 0$ the semiclassical metric is regular and the Kretschmann invariant has a maximum peaked at $r_{\max} \propto l_P$. The radial position of the peak does not depend on the black hole mass and the polymeric parameter δ. The semiclassical solution is very similar to the Reissner-Nordström metric. We construct the Carter-Penrose diagrams explicitly, giving a causal description of the space-time and its maximal extension. The LQBH metric interpolates between two asymptotically *flat* regions, the $r \to \infty$ region and the $r \to 0$ region. We study the thermodynamics of the semiclassical solution. The temperature, entropy and the evaporation process are regular and could be defined independently from the polymeric parameter δ. We study the particular metric when the polymeric parameter goes towards to zero. This metric is regular in $r = 0$ and has only one event horizon in $r = 2m$. The radial position of the Kretschmann invariant maximum depends only on l_P. As such the polymeric parameter δ does not play any role in the black hole singularity resolution. The thermodynamics is the same.

Keywords Black hole · Loop quantum gravity

Introduction

Quantum gravity is the theory attempting to reconcile general relativity and quantum mechanics. In general relativity the space-time is dynamical, therefore it is not possible to study

L. Modesto (✉)
Perimeter Institute for Theoretical Physics, 31 Caroline St., Waterloo, ON N2L 2Y5, Canada
e-mail: lmodesto@perimeterinstitute.ca

other interactions on a fixed background because the background itself is a dynamical field. "loop quantum gravity" (LQG) [1–5] gives as a framework for reconciling general relativity and quantum mechanics. This is one of the non perturbative and background independent approaches to quantum gravity. LQG is a quantum geometric fundamental theory that reconciles general relativity and quantum mechanics at the Planck scale and we expect that this theory could resolve the classical singularity problems of General Relativity. Much progress has been made in this direction in the last years. In particular, the application of LQG technology to the early universe in the context of minisuperspace models have solved the initial singularity problem [6–11].

Black holes are another interesting place for testing the validity of LQG. In the past years applications of LQG ideas to the Kantowski-Sachs space-time [12, 13] lead to some interesting results in this field. In particular, it has been showed [14–20] that it is possible to solve the black hole singularity problem by using tools and ideas developed in the full LQG. Other remarkable results have been obtained in the non homogeneous case [21–23].

There are also works of semiclassical nature which try to solve the black hole singularity problem [24–27]. In these papers the authors use an effective Hamiltonian constraint obtained by replacing the Ashtekar connection A with the holonomy $h(A)$ and they solve the classical Hamilton equations of motion exactly or numerically. In this paper we try to improve the semiclassical analysis introducing a very simple modification to the Hamiltonian constraint expressed in terms of the holonomies. The main result is that the minimum area [28–30] of full LQG is the fundamental ingredient to solve the black hole space-time singularity problem in $r = 0$. The S^2 sphere bounces on the minimum area a_0 of LQG and the singularity disappears. We show that the Kretschmann invariant is regular in all space-time and the position of the maximum is independent of the mass and of the polymeric parameter introduced to define the Hamiltonian constraint in terms of holonomies. The radial position of the curvature maximum depends only on G_N and $\hbar$.

This paper is organized as follows. In the first section we recall the classical Schwarzschild solution in Ashtekar's variables. In the second section we introduce a class of Hamiltonian constraints expressed in terms of holonomies that reduce to the classical one in the limit where the polymer parameter $\delta \to 0$. We solve the Hamilton equations of motion obtaining the semiclassical black hole solution for a particular choice of the quantum constraint. In the third section we show the regularity of the solution by studying the Kretschmann operator and we write the solution in a very simple form similar to the Reissner-Nordström solution for a black hole with mass and charge. In section four we study the space-time structure and we construct the Carter-Penrose diagrams. In section five we show the solution has a Schwarzschild core in $r \to 0^+$. In section six we analyze the black hole thermodynamics by calculating the temperature, entropy and evaporation. In section seven we calculate the limit $\delta \to 0$ of the metric and we obtain a regular semiclassical solution with the same thermodynamic properties but with only one event horizon at the Schwarzschild radius. We analyze the causal space-time structure and construct the Carter-Penrose diagrams.

1 Schwarzschild Solution in Ashtekar Variables

In this section we recall the classical Schwarzschild solution inside the event horizon [14–20]. For the homogeneous but non isotropic Kantowski-Sachs space-time the Ashtekar's variables [31, 60] are

$$\begin{aligned} A &= \tilde{c}\tau_3 dx + \tilde{b}\tau_2 d\theta - \tilde{b}\tau_1 \sin\theta d\phi + \tau_3 \cos\theta d\phi, \\ E &= \tilde{p}_c \tau_3 \sin\theta \frac{\partial}{\partial x} + \tilde{p}_b \tau_2 \sin\theta \frac{\partial}{\partial \theta} - \tilde{p}_b \tau_1 \frac{\partial}{\partial \phi}. \end{aligned} \tag{1}$$

The components variables in the phase space have length dimension $[\tilde{c}] = L^{-1}$, $[\tilde{p}_c] = L^2$, $[\tilde{b}] = L^0$, $[\tilde{p}_b] = L$. The Hamiltonian constraint is

$$\mathcal{C}_H = -\int \frac{N dx \sin\theta d\theta d\phi}{8\pi G_N \gamma^2}\left[(\tilde{b}^2+\gamma^2)\frac{\tilde{p}_b \operatorname{sgn}(\tilde{p}_c)}{\sqrt{|\tilde{p}_c|}} + 2\tilde{b}\tilde{c}\sqrt{|\tilde{p}_c|}\right]. \tag{2}$$

Using the general relation $E^a_i E^b_j \delta^{ij} = \det(q) q^{ab}$ (q_{ab} is the metric on the spatial section) we obtain $q_{ab} = (\tilde{p}_b^2/|\tilde{p}_c|, |\tilde{p}_c|, |\tilde{p}_c|\sin^2\theta)$.

We restrict integration over x to a finite interval L_0 and the Hamiltonian takes the form [19, 20]

$$\mathcal{C}_H = -\frac{N}{2G_N\gamma^2}\left[(b^2+\gamma^2)\frac{p_b \operatorname{sgn}(p_c)}{\sqrt{|p_c|}} + 2bc\sqrt{|p_c|}\right]. \tag{3}$$

The rescaled variables are: $b = \tilde{b}$, $c = L_0\tilde{c}$, $p_b = L_0\tilde{p}_b$, $p_c = \tilde{p}_c$. The length dimensions of the new phase space variables are: $[c] = L^0$, $[p_c] = L^2$, $[b] = L^0$, $[p_b] = L^2$. From the symmetric reduced connection and density triad we can read the components variables in the phase space: (b, p_b), (c, p_c), with Poisson algebra $\{c, p_c\} = 2\gamma G_N$, $\{b, p_b\} = \gamma G_N$. We choose the gauge $N = \gamma\sqrt{|p_c|}\operatorname{sgn}(p_c)/b$ and the Hamiltonian constraint reduce to

$$\mathcal{C}_H = -\frac{1}{2G_N\gamma}\left[(b^2+\gamma^2)p_b/b + 2cp_c\right]. \tag{4}$$

The Hamilton equations of motion are

$$\dot{b} = \{b, \mathcal{C}_H\} = -\frac{b^2+\gamma^2}{2b}, \tag{5}$$

$$\dot{p}_b = \{p_b, \mathcal{C}_H\} = \frac{1}{2}\left[p_b - \frac{\gamma^2 p_b}{b^2}\right], \tag{6}$$

$$\dot{c} = \{c, \mathcal{C}_H\} = -2c, \tag{7}$$

$$\dot{p}_c = \{p_c, \mathcal{C}_H\} = 2p_c. \tag{8}$$

The solutions of those equations using the time parameter $t \equiv \sqrt{p_c^0}e^T$ and redefining the integration constant $\sqrt{p_c^0}e^{T_0} = 2m$ (where p_c^0 is the integration constant of (8), $[p_c^0] = L^2$) [14–20] are

$$\begin{aligned} b(t) &= \pm\gamma\sqrt{(2m/t)-1}, \\ p_b(t) &= p_b^0\sqrt{t(2m-t)}, \\ c(t) &= \mp\gamma m p_b^0 t^{-2}, \\ p_c(t) &= \pm t^2. \end{aligned} \tag{9}$$

($p_b^0 = \tilde{p}_b/\sqrt{p_c^0}$ and $\tilde{p}_b$ is the integration constant for (6), $[\tilde{p}_b] = L^2$) This is exactly the Schwarzschild solution inside and also outside the event horizon as we can verify passing to the metric form defined by $h_{ab} = \operatorname{diag}(p_b^2/|p_c|L_0^2, |p_c|, |p_c|\sin^2\theta)$ (m contains the gravita-

tional constant parameter G_N). The line element is

$$ds^2 = -N^2\frac{dt^2}{t^2} + \frac{p_b^2}{|p_c|L_0^2}dx^2 + |p_c|(\sin^2\theta d\phi^2 + d\theta^2). \tag{10}$$

Introducing the solution (9) in (10) we obtain the Schwarzschild solution in all space-time except in $t = 0$ where the classical curvature singularity is localized and except in $r = 2m$ where there is a coordinate singularity

$$ds^2 = -\frac{dt^2}{\frac{2m}{t} - 1} + \frac{(p_b^0)^2}{L_0^2}\left(\frac{2m}{t} - 1\right)dx^2 + t^2 d\Omega^{(2)}, \tag{11}$$

where $d\Omega^{(2)} = \sin^2\theta d\phi^2 + d\theta^2$. To obtain the Schwarzschild metric we choose $L_0 = p_b^0$. In this way we fix the radial cell to have length p_b^0 and p_b^0 disappears from the metric. In the semiclassical LQBH metric p_b^0 does not disappear fixing L_0. At this level we have not fixed p_b^0 but only the dimension of the radial cell. This is the correct choice to reproduce the Schwarzschild solution metric in all space time. We will do the same choice for the semiclassical metric because in that metric the same coefficients p_b^0/L_0 will appear (this is correct if we want reproduce the Schwarzschild metric at large distances). With this choice p_b^0 will not disappears from the semiclassical metric and in particular from the $p_c(t)$ solution. We will use the minimum area of the full theory to fix p_b^0. For the semiclassical solution at the end of Sect. 4 we will give also a possible physical interpretation of p_b^0.

Another way to eliminate $p_b^0/L_0 \equiv \beta$ is by a coordinate transformation, $x \to x/\beta$. This possibility is viable because the cell volume $L_0 = \int \sqrt{{}^0q}\, dx$, related to the reference spatial metric ${}^0q_{ab} = \mathrm{diag}(1, 1, \sin^2\theta)$, is invariant under a coordinate changing.

2 A General Class of Hamiltonian Constrains

The correct dynamics of loop quantum gravity is the main problem of the theory. LQG is well defined at kinematical level but it is not clear what is the correct version of the Hamiltonian constraint, or more generically, in the covariant approach, what is the correct spin-foam model [32–35]. An empirical principle to construct the correct Hamiltonian constraint is to recall the correct semiclassical limit [36–42]. When we impose spherical symmetry and homogeneity, the connection and density triad assume the particular form given in (1). We can choose a large class of Hamiltonian constraints, expressed in terms of holonomies $h(A; \delta)$, which reduce to the same classical one (4) when the polymeric parameter δ goes to zero. We introduce a parametric function $\sigma(\delta)$ that labels the elements in the class of Hamiltonian constraints compatible with spherical symmetry and homogeneity. We call $\mathcal{C}_{LQG}$ the constrain for the full theory and $\mathcal{C}_{\sigma(\delta)}$ the constraint for the homogeneous spherical minisuperspace model. The reduction from the full LQG classical theory to the minisuperspace model is

$$\mathcal{C}_{LQG} \to \mathcal{C}_{\sigma(\delta)}, \tag{12}$$

where the arrow represents the spherical symmetric reduction of the Hamiltonian constraint. To obtain the classical Hamiltonian constraint (4) in the limit $\delta \to 0$ we recall that the function $\sigma(\delta)$ satisfies the following condition

$$\lim_{\delta\to 0}\sigma(\delta) = 1 \quad \to \quad \lim_{\delta\to 0}\mathcal{C}_{\sigma(\delta)} = \mathcal{C}_H. \tag{13}$$

We are going to show that just one particular choice of $\sigma(\delta)$ gives the correct asymptotic flat limit for the Schwarzschild black hole. In fact the asymptotic *boundary condition* selects the particular form of the function $\sigma(\delta)$. The model we are going to introduce is inspired by LQG, we apply the technology introduced in the full theory to a particular reduced model. Moreover the rigorous mathematical relation between the reduced model and the full theory is an open problem.

The classical Hamiltonian constraint can be written in the following form

$$\mathcal{C}_H = \frac{1}{\gamma^2}\int d^3x \epsilon_{ijk} e^{-1} E^{ai} E^{bj} \big[\gamma^2 \Omega^k_{ab} - {}^0 F^k_{ab}\big], \tag{14}$$

where $\Omega = -\sin\theta\tau_3 d\theta \wedge d\phi$ and ${}^0F = dK + [K, K]$ (K is the extrinsic curvature, $A = \Gamma + \gamma K$ and $\Gamma = \cos\theta\tau_3 d\phi$). The holonomies in the directions x, θ, ϕ for a generic path ℓ are defined by

$$\begin{aligned} h_1^{(\ell)} &= \cos\frac{\ell c}{2} + 2\tau_3 \sin\frac{\ell c}{2}, \\ h_2^{(\ell)} &= \cos\frac{\ell b}{2} + 2\tau_2 \sin\frac{\ell b}{2}, \\ h_3^{(\ell)} &= \cos\frac{\ell b}{2} - 2\tau_1 \sin\frac{\ell b}{2}. \end{aligned} \tag{15}$$

We define the field strength ${}^0F^i_{ab}$ in terms of holonomies in the following way

$$\begin{aligned} {}^0F^i_{ab}\tau_i &= {}^0\omega^i_a\, {}^0\omega^j_b \left(\frac{h_i^{(\delta_i)} h_j^{(\delta_j)} h_i^{(\delta_i)-1} h_j^{(\delta_j)-1} - 1}{\delta^2}\right), \\ \delta_i &= (\delta c, \sigma(\delta)\delta b, \sigma(\delta)\delta b), \end{aligned} \tag{16}$$

where δ_i is the length of the curve along which we integrate the connection; δ is the polymeric parameter (which disappears in the full LQG theory) which we think to be constrained by observations. In the right hand side of the field strength there is no sum over the i, j indexes. It's a simple exercise to verify that when $\delta \to 0$ (16) we obtain the classical field strength. The Hamiltonian constraint in terms of holonomies is

$$\begin{aligned} \mathcal{C}_{\sigma(\delta)} &= \frac{-N}{8\pi G_N^2 \gamma^3 \delta^3} \mathrm{Tr}\Bigg[\sum_{ijk} \epsilon^{ijk} h_i^{(\delta_i)} h_j^{(\delta_j)} h_i^{(\delta_i)-1} h_j^{(\delta_j)-1} h_k^{(\delta)} \big\{h_k^{(\delta)-1}, V\big\} \\ &\quad + 2\gamma^2\delta^2\tau_3 h_1^{(\delta)} \big\{h_1^{(\delta)-1}, V\big\}\Bigg] \\ &= -\frac{N}{2G_N\gamma^2}\left\{2\frac{\sin\delta c}{\delta}\frac{\sin(\sigma(\delta)\delta b)}{\delta}\sqrt{|p_c|} + \left(\frac{\sin^2(\sigma(\delta)\delta b)}{\delta^2} + \gamma^2\right)\frac{p_b \,\mathrm{sgn}(p_c)}{\sqrt{|p_c|}}\right\}. \end{aligned} \tag{17}$$

$V = 4\pi\sqrt{|p_c|}p_b$ is the spatial section volume. We have introduced modifications depending on the function $\sigma(\delta)$ only in the field strength but this is sufficient to have a large class of semiclassical Hamiltonian constraints compatible with spherical symmetry. The Hamiltonian constraint $\mathcal{C}_{\sigma(\delta)}$ in (17) can be substantially simplified in the gauge $N = (\gamma\sqrt{|p_c|}\mathrm{sgn}(p_c)\delta)/(\sin\sigma(\delta)\delta b)$

$$\mathcal{C}_{\sigma(\delta)} = -\frac{1}{2\gamma G_N}\left\{2\frac{\sin\delta c}{\delta}\, p_c + \left(\frac{\sin\sigma(\delta)\delta b}{\delta} + \frac{\gamma^2\delta}{\sin\sigma(\delta)\delta b}\right)p_b\right\}. \tag{18}$$

From (18) we obtain two independent sets of equations of motion on the phase space

$$
\begin{aligned}
\dot{c} &= -2\frac{\sin\delta c}{\delta},\\
\dot{p_c} &= 2p_c\cos\delta c,\\
\dot{b} &= -\frac{1}{2}\left(\frac{\sin\sigma(\delta)\delta b}{\delta}+\frac{\gamma^2\delta}{\sin\sigma(\delta)\delta b}\right),\\
\dot{p_b} &= \frac{\sigma(\delta)}{2}\cos\sigma(\delta)\delta b\left(1-\frac{\gamma^2\delta^2}{\sin^2\sigma(\delta)\delta b}\right)p_b.
\end{aligned}
\tag{19}
$$

Solving the first three equations and using the Hamiltonian constraint $\mathcal{C}_{\sigma(\delta)}$, with the time parametrization $\sqrt{p_c^0}\,e^T = t$ (see the first section about the length units) and imposing to have the Schwarzschild event horizon in $t = 2m$, we obtain

$$
\begin{aligned}
c(t) &= \frac{2}{\delta}\arctan\left(\mp\frac{\gamma\delta m p_b^0}{2t^2}\right),\\
p_c(t) &= \pm\frac{1}{t^2}\left[\left(\frac{\gamma\delta m p_b^0}{2}\right)^2+t^4\right],\\
\cos\sigma(\delta)\delta b(t) &= \rho(\delta)\left[\frac{1-(\frac{2m}{t})^{\sigma(\delta)\rho(\delta)}\mathcal{P}(\delta)}{1+(\frac{2m}{t})^{\sigma(\delta)\rho(\delta)}\mathcal{P}(\delta)}\right],\\
p_b(t) &= -\frac{2\sin\delta c(t)\sin\sigma(\delta)\delta b(t)\,p_c(t)}{\sin^2\sigma(\delta)\delta b(t)+\gamma^2\delta^2},
\end{aligned}
\tag{20}
$$

where in the last relation $p_c(t)\sin\delta c(t)$ is a constant of motion. We have defined also the quantities

$$
\begin{aligned}
\rho(\delta) &= \sqrt{1+\gamma^2\delta^2},\\
\mathcal{P}(\delta) &= \frac{\sqrt{1+\gamma^2\delta^2}-1}{\sqrt{1+\gamma^2\delta^2}+1}.
\end{aligned}
\tag{21}
$$

Now we focus our attention on the term $(2m/t)^{\sigma(\delta)\rho(\delta)}$. The choice of this term and in particular the choice of the exponent will be crucial to have the correct flat asymptotic limit. The exponent is in the form $(2m/t)^{1+\epsilon}$ and expanding in powers of the small parameter $\epsilon \propto \delta^2$ we obtain $(2m/t)^{1+\epsilon} \to -(2m/t)\log(t/2m)$ at large distance ($t \gg 2m$) (we remember that outside the event horizon the coordinate t plays the rule of spatial radial coordinate). It is straightforward to see that there exists only one possible way to obtain the correct asymptotic limit and it is given by the choice $\sigma(\delta) = 1/\sqrt{1+\gamma^2\delta^2}$. In fact only for this choice of $\sigma(\delta)$ the term $\log(t/2m)$ disappears asymptotically for $t \to +\infty$ (t is a spatial coordinate outside the event horizon).

Let as take $\sigma(\delta) = 1/\sqrt{1+\gamma^2\delta^2}$. Since we have the correct large distance limit and because of the regularity of the curvature invariant on all of space-time, we will extend the solution outside the event horizons with the redefinition $t \leftrightarrow r$. We will come back to this extension in the next section.

A crucial difference with the classical Schwarzschild solution is that p_c has a minimum (we consider the plus sign in (20)) in $t_{\min} = (\gamma\delta m p_b^0/2)^{1/2}$, and $p_c(t_{\min}) = \gamma\delta m p_b^0$. The solution has a spacetime structure very similar to the Reissner-Nordström metric and presents

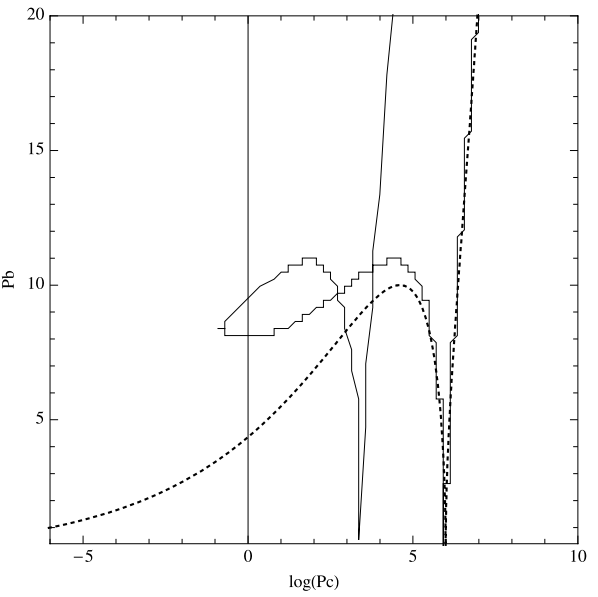

Fig. 1 Semiclassical dynamical trajectory on the plane $(|p_b|/p_b^0, \log(p_c))$ for positive values of p_c. *The dashed trajectory* corresponds to the classical Schwarzschild solution and *the continuum trajectory* corresponds to the semiclassical solution. The plot refers to $m = 10$, $p_b^0 = 1/10$ and $\gamma\delta = \log(4)/\pi$

an inner horizon at

$$r_- = 2m\mathcal{P}(\delta)^2 = 2m\left(\frac{2+\gamma^2\delta^2-2\sqrt{1+\gamma^2\delta^2}}{2+\gamma^2\delta^2+2\sqrt{1+\gamma^2\delta^2}}\right). \tag{22}$$

For $\delta \to 0$, $r_- = m\gamma^4\delta^4/8 + O(\gamma^6\delta^6)$. We observe that the inside horizon position $r_- \neq 2m$ $\forall\gamma \in \mathbb{R}$ (we recall γ is the Barbero-Immirzi parameter). Now we study the trajectory in the plane $(|p_b|/p_b^0, \log(p_c))$ and we compare the result with the Schwarzschild solution. In Fig. 1 we have a parametric plot of $(|p_b|/p_b^0, \log(p_c))$; we can follow the trajectory from $t > 2m$ where the classical (dashed trajectory) and the semiclassical (continuum trajectory) solution are very close. For $t = 2m$, $p_c \to (2m)^2$ and $p_b \to 0$ (this point corresponds to the Schwarzschild radius). From this point decreasing t we reach a minimum value for $p_{c,m} \equiv p_c(t_{\min}) > 0$. From $t = t_{\min}$, p_c starts to grow again until $p_b = 0$, this point corresponds to a new horizon in $t = r_-$ localized. In the time interval $t < t_{\min}$, p_c grows together with $|p_b|$ and as it is very clear from the picture the solution approach the second specular black hole for $t \to 0$. In particular we have a second $flat$ asymptotic region for $t \to 0$.

Metric Form of the Solution

In this section we write the solution in metric form and we extend it analytically to the all space-time. We recall the Kantowski-Sachs metric is $ds^2 = -N^2(t)dt^2 + X^2(t)dx^2 + Y^2(t)(d\theta^2 + \sin\theta d\phi^2)$. The metric components are related to the connection variables by

$$N^2(t) = \frac{\gamma^2\delta^2|p_c(t)|}{t^2\sin^2\sigma(\delta)\delta b}, \qquad X^2(t) = \frac{p_b^2(t)}{L_0^2|p_c(t)|}\Omega(\delta), \qquad Y^2(t) = |p_c(t)|. \tag{23}$$

We have introduced $\Omega(\delta)$ through a coordinate transformation $x \to \sqrt{\Omega(\delta)}\,x$,

$$\Omega(\delta) = 16(1+\gamma^2\delta^2)^2/(1+\sqrt{1+\gamma^2\delta^2})^4. \tag{24}$$

This coordinate transformation is useful to obtain the Minkowski metric in the limit $t \to \infty$. The explicit form of the lapse function $N(t)^2$ in terms of the coordinate t is

$$N^2(t) = \frac{\gamma^2\delta^2[(\frac{\gamma\delta m p_b^0}{2t^2})^2 + 1]}{1 - \rho^2(\delta)[\frac{1-(\frac{2m}{t})\mathcal{P}(\delta)}{1+(\frac{2m}{t})\mathcal{P}(\delta)}]^2}. \tag{25}$$

Using the second relation in (23) we can obtain the $X^2(t)$ metric component,

$$X^2(t) = \frac{(2\gamma\delta m)^2\Omega(\delta)(1 - \rho^2(\delta)[\frac{1-\frac{2m}{t}\mathcal{P}(\delta)}{1+\frac{2m}{t}\mathcal{P}(\delta)}]^2)\, t^2}{\rho^4(\delta)(1 - [\frac{1-\frac{2m}{t}\mathcal{P}(\delta)}{1+\frac{2m}{t}\mathcal{P}(\delta)}]^2)^2[(\frac{\gamma\delta m p_b^0}{2})^2 + t^4]}. \tag{26}$$

The function $Y^2(t)$ corresponds to $|p_c(t)|$ given in (20). The metric obtained has the correct asymptotic limit for $t \to +\infty$ and in fact $N^2(t \to +\infty) \to -1$, $X^2(t \to +\infty) \to -1$, $Y^2(t \to +\infty) \to t^2$. The semiclassical metric goes to a flat limit also for $t \to 0$ by a coordinate changing that we will introduce in Sect. 4. We can say that LQBH interpolates between two asymptotic flat region of the space-time. The metric obtained in this paper has the correct flat asymptotic limit for $t \to +\infty$ and reproduce the Minkowski metric for $m \to 0$. Those limit are not both satisfied in [24, 25]. The small modification introduced in the holonomy form of the Hamiltonian is necessary for those two fundamental consistency limit.

3 LQBH in All Space-Time

In this section we extend the semiclassical (metric) solution obtained in the previous section to all space-time. As explained in the previous subsection the metric solution has the correct flat limit for $t \to +\infty$ and goes to Minkowski for $m \to 0$. Now we see that the Kretschmann scalar $K = \mathrm{R}_{\mu\nu\rho\sigma}\mathrm{R}^{\mu\nu\rho\sigma}$ is regular in all space-time. In terms of $N(t)$, $X(t)$ and $Y(t)$ the Kretschmann scalar is

$$\begin{aligned}\mathrm{R}_{\mu\nu\rho\sigma}\mathrm{R}^{\mu\nu\rho\sigma} = 4\Bigg[&\left(\frac{1}{XN}\frac{d}{dt}\left(\frac{1}{N}\frac{dX}{dt}\right)\right)^2 + 2\left(\frac{1}{YN}\frac{d}{dt}\left(\frac{1}{N}\frac{dY}{dt}\right)\right)^2 \\ &+ 2\left(\frac{1}{XN}\frac{dX}{dt}\frac{1}{YN}\frac{dY}{dt}\right)^2 + \frac{1}{Y^4N^4}\left(N^2 + \left(\frac{dY}{dt}\right)^2\right)^2\Bigg].\end{aligned} \tag{27}$$

In Fig. 2 is plotted a graph of K, it is regular in all space-time and the large t behavior is the classical singular scalar $\mathrm{R}_{\mu\nu\rho\sigma}\mathrm{R}^{\mu\nu\rho\sigma} = 48m^2/t^6$.

What about p_b^0? We fix the parameter p_b^0 using the full theory (LQG). In particular we choose p_b^0 in such way that the position t_{Max} of the Kretschmann invariant maximum is independent of the black hole mass. This means the S^2 sphere bounces on a minimum radius that is independent of the mass of the black hole and independent of p_b^0 and depends only on l_P. We consider the solution $p_c(t)$ and we impose the minimum area $A_{\mathrm{Min}} = 4\pi\gamma\delta m p_b^0$ of the S^2 sphere to be equal to the minimum gap area of loop quantum gravity $a_0 = 4\pi\sqrt{3}\gamma l_P^2$. With the choice $\gamma\delta m p_b^0 = a_0/4\pi$ we obtain a significant physical result. We have *not* impose $p_c(t)$ to have a minimum in a_0 but we have just impose that the minimum of $p_c(t)$ is the minimum area of the full theory. The minimum area of the two sphere is a result and not

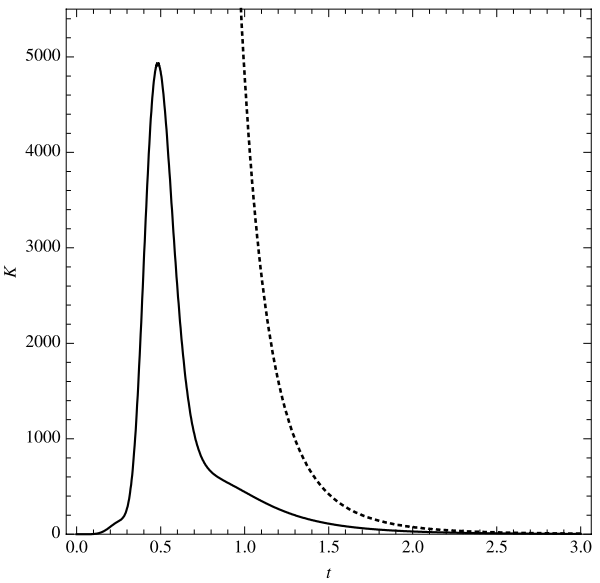

Fig. 2 Plot of the Kretschmann scalar invariant $R_{\mu\nu\rho\sigma}R^{\mu\nu\rho\sigma}$ for $m = 10$, $p_b^0 = 1/10$ and $\gamma\delta = \log(4)/\pi$, $\forall t \geq 0$; the large t behaviour is $1/t^6$

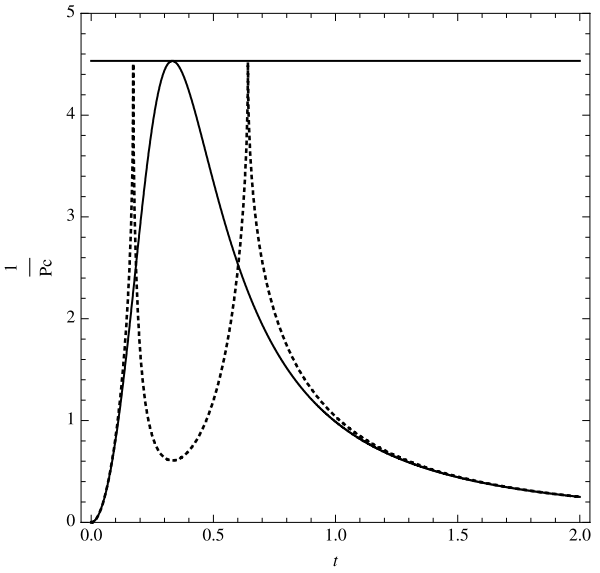

Fig. 3 Plot of the spectrum of the operator $\widehat{1/|p_c|}$ evaluated on $\tau\gamma = p_c(t)$ (where τ is the eigenvalue of the operator $\hat{p}_c$: $\hat{p}_c|\tau\rangle = \gamma l_P^2 \tau|\tau\rangle$) (*dashed line*) compared with the semiclassical solution $1/p_c(t)$ itself (*solid line*)

a requirement. We observe that this choice of p_b^0 fixes the absolute maximum and relative minimum of $p_b(t)$ to be independent of the mass m as is manifest from the plot in Fig. 4.

We can also fix the parameter p_b^0 without making use of the minimum area gap of the full theory. The idea is to compare the spectrum of the operator $\widehat{1/|p_c|}$ [24, 25] with the semiclassical solution $1/p_c(t)$ (Fig. 3). More precisely we identify the max eigenvalue of $\widehat{1/|p_c|}$ with the max of the function $1/p_c(t)$. The result is $mp_b^0 = l_P^2/2$ and then $A_{\text{Min}} = 4\pi\sqrt{3}\gamma l_P^2$

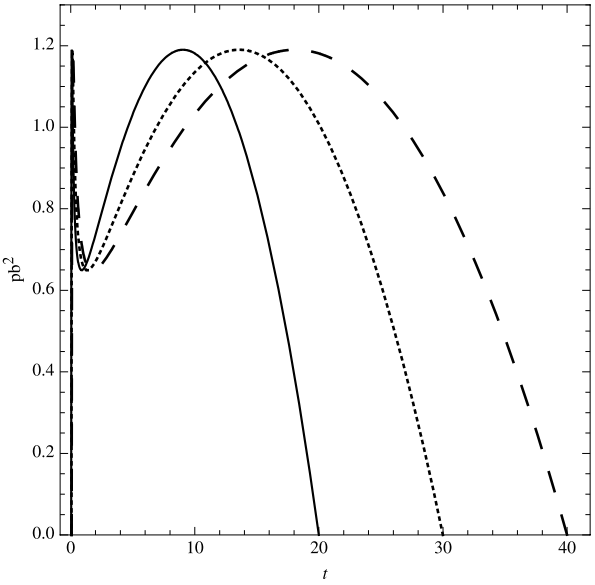

Fig. 4 Plot of $p_b^2(t)$ for different values of the mass ($m = 10, 15, 20$). Max (absolute) and Min (relative) of $p_b^2(t)$ are independent of the mass m

for $\delta = 2\sqrt{3}$ [19, 20]. The minimum area obtained in the minisuperspace framework without making use of the full theory is exactly the minimum area of full LQG.

We want to provide a heuristic argument to support the choice $p_b^0 \propto a_0/m$. In the papers [43–46] it is shown that the phase space is parametrized by m and the conjugate momentum p_m and it is shown that are both constants of motion (in our notation $p_m = p_b^0$). As is usually done in elementary quantum mechanics to derive the Heisenberg uncertainty relation, we can introduce the state $|\phi\rangle = (\hat{m} + i\lambda\hat{p}_m)|\psi\rangle$, where $\hat{m}$ and $\hat{p}_m$ are the mass and momentum operators and $\lambda \in \mathbb{R}$. From the positive norm $\langle\phi|\phi\rangle = \langle\hat{m}^2\rangle + i\lambda\langle[\hat{m}, \hat{p}_m]\rangle + \lambda^2\langle\hat{p}_m^2\rangle \geq 0$ we have the discriminant, of second order in λ, is negative or zero. The condition on the discriminant gives $\langle\hat{m}^2\rangle\langle\hat{p}_m^2\rangle \geq -\langle[\hat{m}, \hat{p}_m]\rangle^2/4$. Introducing the commutator $[\hat{m}, \hat{p}_m] = il_P^2$ we obtain $\langle\hat{m}^2\rangle\langle\hat{p}_m^2\rangle \geq l_P^4/4$. We can calculate $\langle\hat{m}^2\rangle$ on semiclassical Gaussian states,

$$\Psi(m)_{m_0,p_0} = \frac{\mathrm{e}^{-\frac{(m-m_0)^2}{4(\Delta m)^2}}\,\mathrm{e}^{\frac{ip_0 m}{l_P^2}}}{[2\pi(\Delta m)^2]^{1/4}}, \tag{28}$$

and the result is $\langle\hat{m}^2\rangle = m_0^2 + (\Delta m)^2$. Using the Heisenberg uncertainty relation, $\langle\hat{m}^2\rangle = m_0^2 + (\Delta m)^2 := m^2$ and $\langle\hat{p}_m^2\rangle = p_0^2 + (\Delta p_m)^2 := (p_b^0)^2$, we obtain $mp_b^0 \geq l_P^2/2$, which is exactly $mp_b^0 \geq a_0/4\pi\gamma\delta$ for $\delta = 2\sqrt{3}$, $a_0 = 4\pi\sqrt{3}\gamma l_P^2$. We have introduced explicitly all the coefficients but the main result is $p_b^0 \propto a_0/m$. What is presented here is just a heuristic argument (not a proof) that includes a number of not so obvious hypotheses, however it shows our choice of p_b^0 is consistent with [43–46].

At the end of Sect. 4 we will give a physical interpretation of p_b^0.

We now want underline the similarity between the equation of motion for $p_c(t)$ and the Friedmann equation of loop quantum cosmology. We can write the differential equation for $p_c(t)$ in the following form

$$\left(\frac{\dot{p}_c}{p_c}\right)^2 = 4\left(1 - \frac{a_0^2}{16\pi^2 p_c^2}\right). \tag{29}$$

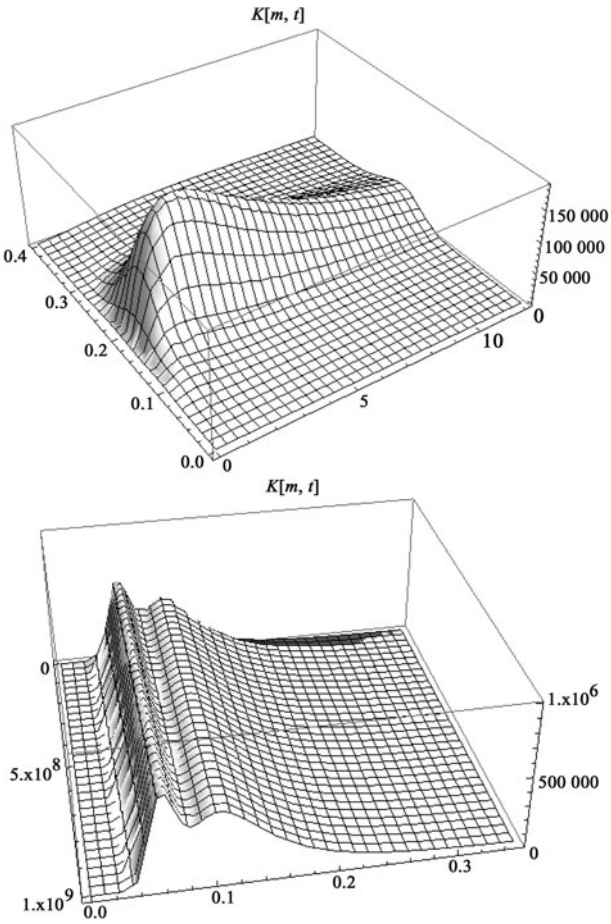

Fig. 5 Plot of the Kretschmann invariant $R_{\mu\nu\rho\sigma}R^{\mu\nu\rho\sigma}(m,t)$ for $m \in [0, 10^6]$, $t \in [0, 0.4]$ $\gamma\delta = \log(4)/\pi$. *The first plot* represents the Kretschmann invariant for small values of m and *the second* for $m \in [0, 10^6]$, the variable t is in the range $[0, 0.4]$

From this equation is manifest that p_c bounces at the value $a_0/4\pi$. This is quite similar to the loop quantum cosmology bounce [48].

As is evident from Fig. 5 the maximum of the Kretschmann invariant is independent of the mass and is localized in $t_{\text{Max}} \propto \sqrt{a_0}(a_0 \propto l_P^2)$. At this point we redefine the variables $t \leftrightarrow x$ (with the subsequent identification $x \equiv r$) to bring the solution in the standard Schwarzschild form

$$\begin{aligned} -N^2(t) &\to g_{rr}(r), \\ X^2(t) &\to g_{tt}(r), \\ Y^2(t) &\to g_{\theta\theta}(r) = g_{\phi\phi}/\sin^2\theta. \end{aligned} \tag{30}$$

Schematically the properties of the metric are the following,

- $\lim_{r\to+\infty} g_{\mu\nu}(r) = \eta_{\mu\nu}$,
- $\lim_{r\to 0} g_{\mu\nu}(r) = \eta_{\mu\nu}$,

$$\begin{aligned} &\bullet \lim_{m,a_0\to 0} g_{\mu\nu}(r) = \eta_{\mu\nu}, \\ &\bullet K(g) < \infty, \quad \forall r, \\ &\bullet r_{\mathrm{Max}}(K(g)) \propto \sqrt{a_0}. \end{aligned} \tag{31}$$

In Sect. 5 we will explicitly introduce the coordinates which remove the coordinate singularities on the event horizons and we will show the metric can be continued analytically to all of space-time. We consider these properties sufficient to extend the solution in all space-time. The solution is summarized in Table 1 (in the table we have not fixed the parameter p_b^0).

We have said in the previous section that the metric solution has two event horizons. An event horizon is defined [47] by a null surface $\Sigma(r,\theta) = \text{const.}$ which extends to spatial infinity. The surface $\Sigma(t,r,\theta,\phi) = \text{const.}$ is a null surface if the normal $n_i = \partial\Sigma/\partial x^i$ is a null vector, if it satisfies the condition $n_i n^i = 0$. The last identity says that the vector n^i is on the surface $\Sigma(t,r,\theta,\phi)$ itself, in fact $d\Sigma = dx^i \partial\Sigma/\partial x^i$ and $dx^i \| n^i$. The norm of the vector n_i is given by

$$n_i n^i = g^{ij} \frac{\partial\Sigma}{\partial x^i} \frac{\partial\Sigma}{\partial x^i} = 0. \tag{32}$$

In our case (32) reduces to

$$g^{rr} \frac{\partial\Sigma}{\partial r} \frac{\partial\Sigma}{\partial r} + g^{\theta\theta} \frac{\partial\Sigma}{\partial\theta} \frac{\partial\Sigma}{\partial\theta} = 0, \tag{33}$$

and this equation is satisfied where $g^{rr}(r) = 0$ if the surface is independent from θ, $\Sigma(r,\theta) = \Sigma(r)$. The points where $g^{rr} = 0$ are r_- and $r_+ = 2m$.

We can write the metric in another form which is similar to the Reissner-Nordström space-time:

$$\begin{aligned} ds^2 = &-\frac{64\pi^2(r-r_+)(r-r_-)(r+r_+\mathcal{P}(\delta))^2}{64\pi^2 r^4 + a_0^2} dt^2 \\ &+ \frac{dr^2}{\frac{64\pi^2(r-r_+)(r-r_-)r^4}{(r+r_+\mathcal{P}(\delta))^2(64\pi^2 r^4 + a_0^2)}} + \left(\frac{a_0^2}{64\pi^2 r^2} + r^2\right) d\Omega^{(2)}. \end{aligned} \tag{34}$$

If we expand the metric (34) in the parameter δ and the minimum area a_0 at the first order we obtain the Schwarzschild solution: $g_{tt}(r) = -(1 - 2m/r) + O(\delta^2) + O(a_0^2)$, $g_{rr}(r) =$

Table 1 Loop quantum black hole in the standard Schwarzschild's metric form

$g_{\mu\nu}$	LQBH	Classical
$g_{tt}(r)$	$\frac{\frac{(2\gamma\delta m)^2\Omega(\delta)}{\rho^4(\delta)}\,(1-\rho^2(\delta)(\frac{1-\frac{2m}{r}\mathcal{P}(\delta)}{1+\frac{2m}{r}\mathcal{P}(\delta)})^2)}{(1-(\frac{1-\frac{2m}{r}\mathcal{P}(\delta)}{1+\frac{2m}{r}\mathcal{P}(\delta)})^2)^2[(\frac{\gamma\delta m p_b^0}{2r})^2+r^2]}$	$-(1-\frac{2m}{r})$
$g_{rr}(r)$	$-\frac{\gamma^2\delta^2[(\frac{\gamma\delta m p_b^0}{2r^2})^2+1]}{1-\rho^2(\delta)(\frac{1-\frac{2m}{r}\mathcal{P}(\delta)}{1+\frac{2m}{r}\mathcal{P}(\delta)})^2}$	$\frac{1}{1-\frac{2m}{r}}$
$g_{\theta\theta}(r)$	$(\frac{\gamma\delta m p_b^0}{2r})^2 + r^2$	r^2

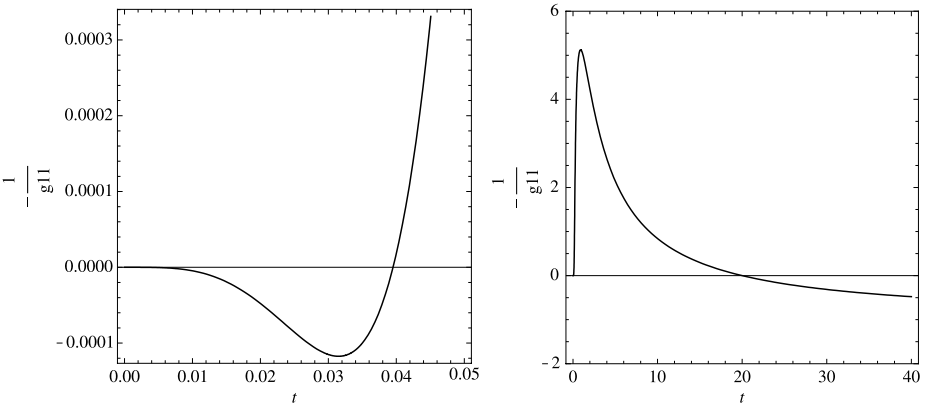

Fig. 6 Plot of $-1/g_{rr}$ for $r \in [0, \approx r_-]$ (*in the first picture*) and $-1/g_{rr}$ for $r \in [\approx r_-, \infty[$ (*in the second picture*). In the plot $g_{11} \equiv g_{rr}$

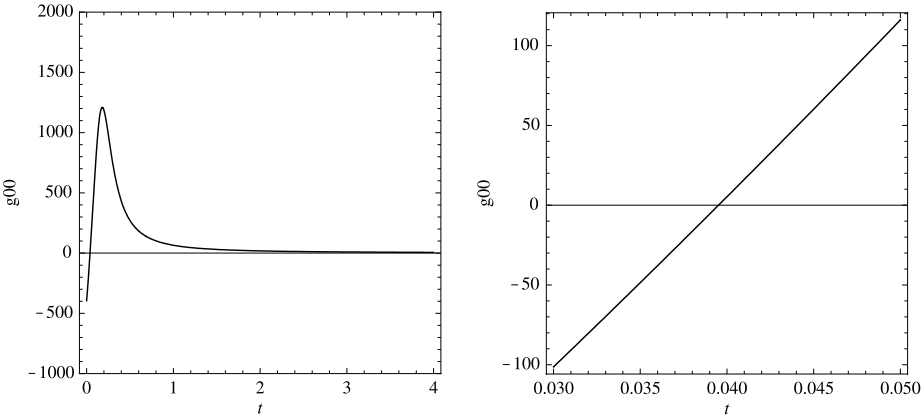

Fig. 7 Plot of g_{tt} for $r \in [0, \approx r_-]$ (*in the first picture*) and g_{tt} for $r \in [\approx r_-, \infty[$ (*in the second picture*). For $r \to 0$ (and small δ), $g_{tt} \to -4m^4\pi^2\gamma^8\delta^8/a_0^2$. In the plot $g_{00} \equiv g_{tt}$

$1/(1-2m/r) + O(\delta^2) + O(a_0^2)$ and $g_{\theta\theta}(r) = g_{\phi\phi}(r)/\sin^2\theta = r^2 + O(a_0^2)$. We have second order correction to the metric from the polymer parameter δ and also from the minimum area a_0.

To check the semiclassical limit we calculate the perturbative expansion of the curvature invariant for small δ and a_0 and we obtain a divergent quantity in $r = 0$ at any order of the development. The regularity of K is a non perturbative result, in fact for small values of the radial coordinate r, $K = 3145728\pi^4 r^6/a_0^4\gamma^8\delta^8 m^2 + O(r^7)$ diverges for $a_0 \to 0$. (For the semiclassical solution the trace of the Ricci tensor ($\mathrm{R} = \mathrm{R}^{\mu}_{\mu}$) is not identically zero as for the Schwarzschild solution. We have also calculated this operator and we have obtained a regular quantity in $r = 0$.) We conclude this section showing the independence of the peak position of Kretschmann invariant from the polymeric parameter δ. We have plotted the invariant $K(\delta, r)$ and we have obtained the result in Fig. 8. From the picture is evident that the position of the Kretschmann's invariant maximum is independent of δ.

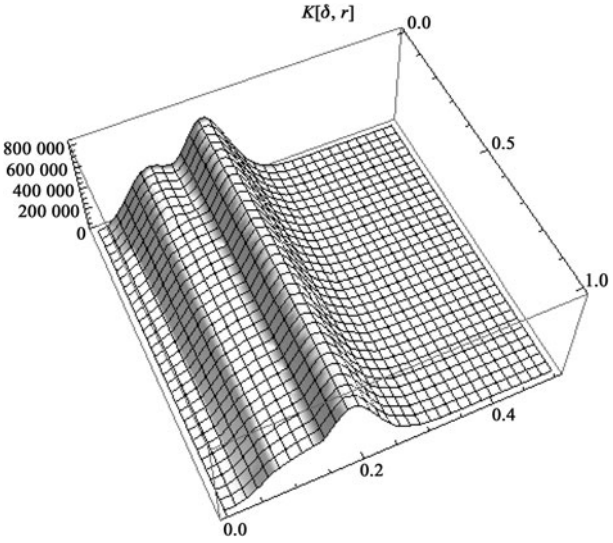

Fig. 8 Plot of the Kretschmann invariant as function of $r \in [0, 0.5]$ and the polymeric parameter $\delta \in [0, 1]$

Corrections to the Newtonian Potential In this paper we are interested in the singularity problem of black hole physics and not in the Post-Newtonian approximation, however we want give the first correction to the gravitational potential. The gravitational potential is related to the metric through $\Phi(r) = -(g_{tt}(r) + 1)/2$. Developing the g_{tt} component of the metric in power of $1/r$ to the order $O(r^{-7})$, for fixed values of the parameter δ and the minimal gap area a_0, we obtain the potential

$$\begin{aligned}\Phi(r) = &-\frac{m}{r}(\mathcal{P}-1)^2 - \frac{4m^2}{r^2}\mathcal{P}(\mathcal{P}^2-\mathcal{P}+1)\\ &-\frac{4m^3}{r^3}(\mathcal{P}-1)^2\mathcal{P}^2 + \left(8m^4\mathcal{P}^4 - \frac{a_0^2}{128\pi^2}\right)\frac{1}{r^4}\\ &+\frac{ma_0^2(\mathcal{P}-1)^2}{64\pi^2 r^5} + \frac{m^2a_0^2\mathcal{P}(1-\mathcal{P}+\mathcal{P}^2)}{16\pi^2 r^6} + O(r^{-7}),\end{aligned} \tag{35}$$

where $\mathcal{P} \equiv \mathcal{P}(\delta)$ is defined in (21).

4 Asymptotic Schwarzschild Core Near $r = 0$

In this section we study the $r \to 0$ limit of the metric (34). If we develop the metric very close to the point $r = 0$ we obtain:

$$ds^2 = -(a - b\,r)dt^2 + \frac{dr^2}{c\,r^4 - d\,r^5} + \frac{d\Omega^{(2)}}{cr^2}. \tag{36}$$

The parametric functions a, b, c, d are

$$\begin{aligned}a &= \frac{64\Omega(\delta)m^4\pi^2\gamma^4\delta^4\mathcal{P}(\delta)^2}{a_0^2(1+\gamma^2\delta^2)^2},\\ b &= \frac{128\Omega(\delta)m^3\pi^2\gamma^2\delta^2\mathcal{P}(\delta)}{a_0^2(1+\gamma^2\delta^2)^2},\end{aligned} \tag{37}$$

$$c = \frac{64\pi^2}{a_0^2},$$
$$d = \frac{128\pi^2(1+\gamma^2\delta^2)}{a_0^2 m\gamma^2\delta^2\mathcal{P}(\delta)}.$$

We consider the coordinate changing $R = 1/r\sqrt{c}$, $t \to \sqrt{a}\,t$. The point $r = 0$ is mapped in the point $R = +\infty$. The metric in the new coordinates is

$$ds^2 = -\left(1 - \frac{m_1}{R}\right)dt^2 + \frac{dR^2}{1-\frac{m_2}{R}} + R^2 d\Omega^{(2)}, \tag{38}$$

where m_1 and m_2 are functions of m, a_0, δ, γ,

$$\begin{aligned} m_1 &= \frac{b}{a\sqrt{c}} = \frac{a_0}{4\pi m\gamma^2\delta^2\mathcal{P}(\delta)}, \\ m_2 &= \frac{d}{c^{3/2}} = \frac{a_0(1+\gamma^2\delta^2)}{4\pi m\gamma^2\delta^2\mathcal{P}(\delta)}. \end{aligned} \tag{39}$$

For small δ we obtain $m_1 = m_2 + O(\delta^2)$ and (38) converges to the Schwarzschild metric of mass $M = a_0/(8\pi m\gamma^2\delta^2\mathcal{P}(\delta)) + O(\delta^2)$. We can conclude the space-time near the point $r = 0$ is described by an effective Schwarzschild metric of mass $M \propto a_0/m$ in the large distance limit $R \gg M$. An observer in the asymptotic region close to the point $r = 0$ experiments a Schwarzschild metric of mass $M \propto a_0/m$.

We now want give a possible physical interpretation of p_b^0. If we reintroduce $p_b^0 \propto a_0/m$ in the *core mass* M defined above we obtain $M \propto p_b^0$, then *we can interpret* p_b^0 *as the mass of the black hole as it is seen by an observer close to* $r = 0$. In [26] the authors interpret p_b^0 as the mass of a second black hole, in our analysis instead p_b^0 seems to be the mass of the black hole but from the point of view of an observer in the asymptotic region $r \to 0$.

5 Causal Structure and Carter-Penrose Diagram

In this section we construct the Carter-Penrose diagrams [49] for the semiclassical metric (34) omitting the S^2 sphere. To obtain the diagrams we will do many coordinate changes and we enumerate them from one to eight.

(1) We can put the metric (34) in the form $ds^2 = g_{00}(r(r^*))(dt^2 - dr^{*2})$ (we do not consider the angular part of the metric) introducing the tortoise coordinate r^* defined by:

$$\begin{aligned} r^* &= \int \sqrt{-\frac{g_{11}}{g_{00}}}dr \\ &= \frac{1}{512\pi^2}\left[-\frac{2a_0^2}{\mathcal{P}(\delta)^2 m^2 r} + 512\pi^2 r + \frac{a_0^2(\mathcal{P}(\delta)^2+1)}{\mathcal{P}(\delta)^4 m^3}\log(r)\right. \\ &\quad \left. - \frac{a_0^2 + 1024\pi^2 m^4}{(\mathcal{P}(\delta)^2-1)m^3}\log|r-r_+| + \frac{a_0^2 + 1024\pi^2\mathcal{P}(\delta)^8 m^4}{(\mathcal{P}(\delta)^2-1)\mathcal{P}(\delta)^4 m^3}\log|r-r_-|\right]. \end{aligned} \tag{40}$$

(2) The second coordinate set to use is (u, v, θ, ϕ), where $u = t - r^*$ and $v = t + r^*$. The metric becomes $ds^2 = g_{00}(u, v)dudv$.

(3) The singularity on the event horizon r_+ disappears using the coordinates (U^+, V^+, θ, ϕ) defined by $U^+ = -\exp(-k_+u)/k_+$, $V^+ = \exp(k_+v)/k_+$, where

$$k_+ = \frac{256\pi^2(1-\mathcal{P}(\delta)^2)m^3}{(a_0^2+1024\pi^2m^4)}. \tag{41}$$

We introduce also the parametric function

$$k_- = \frac{256\pi^2(\mathcal{P}(\delta)^2-1)\mathcal{P}(\delta)^4m^3}{(a_0^2+1024\pi^2\mathcal{P}(\delta)^8m^4)}. \tag{42}$$

Note that $k_+ > 0$ and $k_- < 0$. In those coordinates the metric is

$$\begin{aligned} ds^2 &= -\frac{64\pi^2(r+r_+\mathcal{P}(\delta))^2}{64\pi^2r^4+a_0^2}(r-r_-)^{1-\frac{k_+}{k_-}} \\ &\quad \times \mathrm{e}^{-\frac{k_+}{256\pi^2}[-\frac{2a_0^2}{\mathcal{P}(\delta)^2m^2r}+512\pi^2r+\frac{a_0^2(\mathcal{P}(\delta)^2+1)}{\mathcal{P}(\delta)^4m^3}\log(r)]}dU^+dV^+ \\ &= -F(r)^2dU^+dV^+, \end{aligned} \tag{43}$$

where we have introduced the function $F(r)^2 = -g_{00}(r)(\partial u/\partial U^+)(\partial v/\partial V^+)$ which is defined implicitly in terms of U^+ and V^+.

(4) Using coordinate (t', x', θ, ϕ) defined by $x' = (U^+ - V^+)/2$, $t' = (U^+ + V^+)/2$, the metric (43) assumes the conformally flat form $ds^2 = F(r)^2(-dt'^2 + dx'^2)$. In those coordinates the trajectories of constant r-coordinate are

$$\begin{aligned} U^+V^+ = t'^2 - x'^2 &= -\frac{\mathrm{e}^{2k_+r^*}}{k_+^2} \\ &= -\frac{1}{k_+^2}(r-r_+)(r-r_-)^{\frac{k_+}{k_-}} \\ &\quad \times \mathrm{e}^{\frac{k_+}{256\pi^2}[-\frac{2a_0^2}{\mathcal{P}(\delta)^2m^2r}+512\pi^2r+\frac{a_0^2(\mathcal{P}(\delta)^2+1)}{\mathcal{P}(\delta)^4m^3}\log(r)]}. \end{aligned} \tag{44}$$

The event horizons r_+ and r_- are localized in

$$\begin{aligned} &U^+V^+ = t'^2 - x'^2 = 0, \quad r = r_+, \\ &U^+V^+ = t'^2 - x'^2 \to +\infty, \quad r = r_-. \end{aligned} \tag{45}$$

(5) A first Carter-Penrose diagram for the region $r > r_-$ can be construct using coordinates $(\psi, \xi, \theta, \phi)$ defined by $U^+ \propto \tan[(\psi-\xi)/2]$, $V^+ \propto \tan[(\psi+\xi)/2]$ and $-\pi \le \psi \le \pi$, $-\pi \le \xi \le \pi$. The event horizon $r = r_+$ is localized in $U^+V^+ = 0$ or $\psi = \pm\xi$. The event horizon $r = r_-$ is localized in $U^+V^+ = +\infty$ or: $\psi = \pm\xi \pm \pi$ for $-\pi/2 \le \xi \le 0$, $\psi = \mp\xi \pm \pi$ for $0 \le \xi \le \pi/2$. The other asymptotic regions are: I^+, I^- $(\psi = \mp\xi \pm \pi)$, i^0 $(\psi = 0, \xi = \pi)$, i^+ $(\psi = \pi/2, \xi = \pi/2)$, i^- $(\psi = -\pi/2, \xi = \pi/2)$. The Carter-Penrose diagram for this region is given in the picture on the left in Fig. 9.

(6) In the coordinates introduced above, the metric (34) is not regular in r_-. To remove the singularity in r_- we introduce the coordinates (U^-, V^-, θ, ϕ) defined by $U^- =$

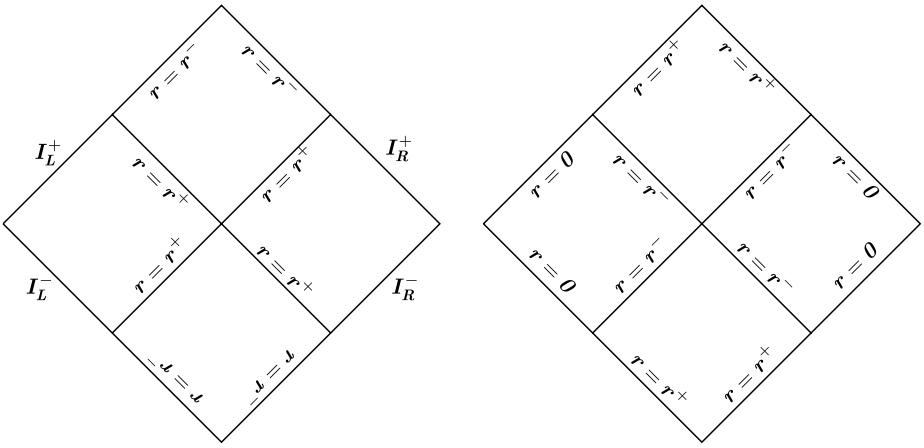

Fig. 9 The picture *on the left* represents the Carter-Penrose diagram in the region outside r_- and the picture *on the right* the diagram for $r_- \leq r \leq 0$

$-\exp(-k_- u)/k_-$, $V^- = \exp(k_- v)/k_-$. In those coordinates the metric is

$$\begin{aligned} ds^2 &= -\frac{64\pi^2(r + r_+\mathcal{P}(\delta))^2}{64\pi^2 r^4 + a_0^2}(r_+ - r)^{1-\frac{k_-}{k_+}} \\ &\quad \times \mathrm{e}^{-\frac{k_-}{256\pi^2}[-\frac{2a_0^2}{\mathcal{P}(\delta)^2 m^2 r} + 512\pi^2 r + \frac{a_0^2(\mathcal{P}(\delta)^2+1)}{\mathcal{P}(\delta)^4 m^3}\log(r)]} dU^- dV^- \\ &= -F'(r)^2 dU^- dV^-, \end{aligned} \tag{46}$$

where $F'(r)^2 = -g_{00}(r)(\partial u/\partial U^-)(\partial v/\partial V^-)$. Now the metric is regular in $r = r_-$ but singular in $r = r_+$.

(7) As in the region $r > r_-$ we introduce coordinates (t'', x'', θ, ϕ) in terms of which $ds^2 = F'^2(r)(-dt''^2 + dx''^2)$. The r-constant trajectories are defined by the curves

$$\begin{aligned} U^- V^- &= t''^2 - x''^2 \\ &= -\frac{1}{k_-^2}(r_- - r)(r_+ - r)^{\frac{k_-}{k_+}} \mathrm{e}^{\frac{k_-}{256\pi^2}[-\frac{2a_0^2}{\mathcal{P}(\delta)^2 m^2 r} + 512\pi^2 r + \frac{a_0^2(\mathcal{P}(\delta)^2+1)}{\mathcal{P}(\delta)^4 m^3}\log(r)]}. \end{aligned} \tag{47}$$

In particular the horizons r_+, r_- and the point $r = 0$ are defined by the curves

$$\begin{aligned} &U^- V^- = t''^2 - x''^2 \to +\infty, \quad r = r_+, \\ &U^- V^- = t''^2 - x''^2 = 0, \quad r = r_-, \\ &U^- V^- = t''^2 - x''^2 \to -\infty, \quad r = 0. \end{aligned} \tag{48}$$

(8) In terms of the coordinates $(\psi', \xi', \theta, \phi)$ defined by $U^- \propto \tan[(\psi' - \xi')/2]$, $V^+ \propto \tan[(\psi' + \xi')/2]$. The event horizon $r = r_-$ is localized in $U^- V^- = 0$ or $\psi' = \pm\xi'$, The event horizon $r = r_+$ is localized in $U^- V^- = +\infty$ or: $\psi' = \mp\xi' \pm \pi$ for $0 \leq \xi' \leq \pi/2$, $\psi' = \pm\xi' \pm \pi$ for $0 \leq \xi' \leq \pi/2$. The other asymptotic regions are defined by $r = 0$: $\psi' = \pm\xi' \mp \pi$ for $\pi/2 \leq \xi \leq \pi$ and $\psi' = \pm\xi' \pm \pi$ for $-\pi \leq \xi' \leq -\pi/2$. The Carter-Penrose diagram for this region is the picture on the right in Fig. 9 (see at the end of this section for the maximal extension of the solution).

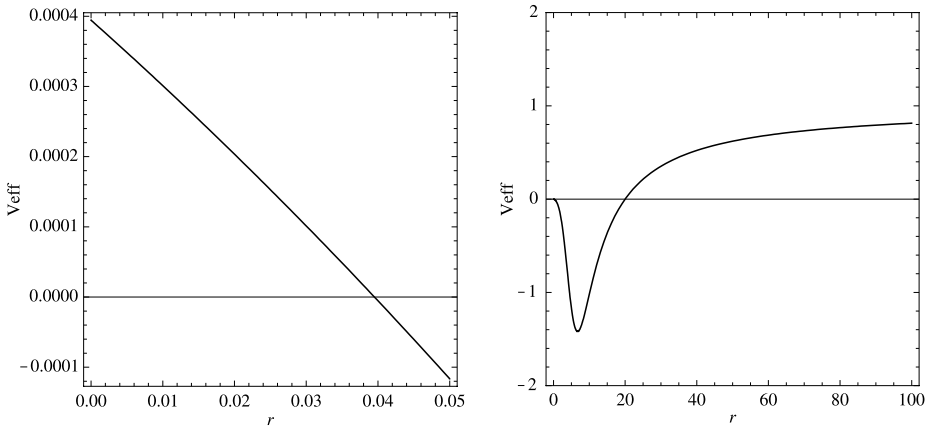

Fig. 10 Plot of $V_{\text{eff}}(r)$. *On the left* there is a zoom of V_{eff} for $r \approx 0$

Now we are going to show that any massive particle could not fall in $r = 0$ in a finite proper time. We consider the radial geodesic equation for a massive point particle

$$(-g_{tt}\, g_{rr})\dot{r}^2 = E_n^2 + g_{tt}, \tag{49}$$

where "˙" is the proper time derivative and E_n is the point particle energy. If the particle falls from the infinity with zero initial radial velocity the energy is $E_n = 1$. We can write (49) in a more familiar form

$$\underbrace{(-g_{tt}\, g_{rr})}_{\geq 0\ \forall r}\dot{r}^2 + \underbrace{V_{\text{eff}}}_{-g_{tt}}(r) = \underbrace{E}_{E_n^2}. \tag{50}$$

A plot of V_{eff} is in Fig. 10. For $r = 0$, $V_{\text{eff}}(r = 0) = 4m^4\pi^2\gamma^8\delta^8/a_0^2$ (for small δ) then any particle with $E < V_{\text{eff}}(0)$ could not arrive in $r = 0$. If the particle energy is $E > V_{\text{eff}}(0)$, the geodesic equation for $r \to 0$ is $\dot{r}^2 \propto r^4$ and integrating $\tau \propto 1/r - 1/r_0$ or $\Delta\tau \equiv \tau(0) - \tau(r_0) \to +\infty$. We can compose the diagrams in Fig. 9 to obtain a maximal extension similar to the Reissner-Nordström one, the result is represented in Fig. 11.

6 LQBH Thermodynamics

In this section we study the thermodynamics of the LQBH [51–57]. The form of the metric calculated in the previous section has the general form

$$ds^2 = -g(r)dt^2 + \frac{dr^2}{f(r)} + h^2(r)(d\theta^2 + \sin^2\theta d\phi^2), \tag{51}$$

where the functions $f(r)$, $g(r)$ and $h(r)$ depend on the mass parameter m and are the components of the metric (34). We can introduce the null coordinate v to express the metric (51) in the Bardeen form. The null coordinate v is defined by the relation $v = t + r^*$, where

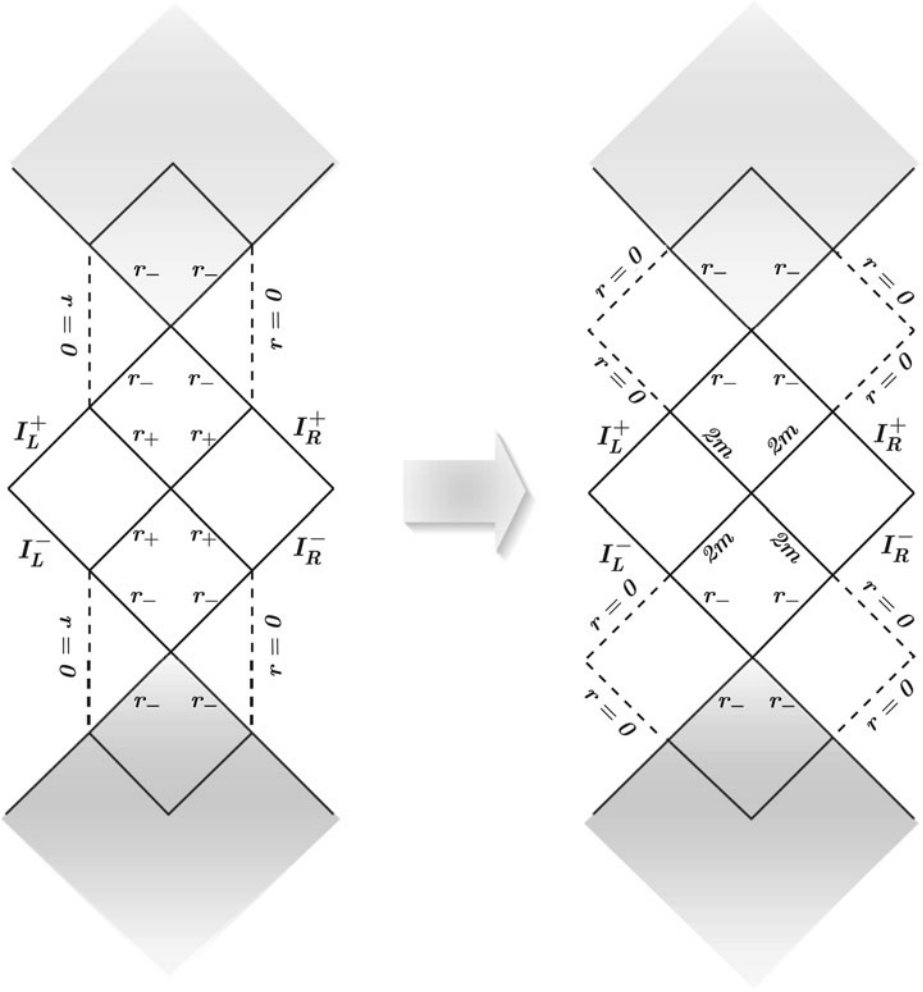

Fig. 11 Maximal space-time extension of the LQBH *on the right* and the analog extension for the Reissner-Nordström black hole *on the left*. The maximal extension is obtained by a superimposition of the two diagrams in Fig. 9 on the sheared region $r_- \leq r \leq r_+ = 2m$

$r^* = \int^r dr/\sqrt{f(r)g(r)}$ and the differential is $dv = dt + dr/\sqrt{f(r)g(r)}$. In the new coordinate the metric is

$$ds^2 = -g(r)dv^2 + 2\sqrt{\frac{g(r)}{f(r)}}\,drdv + h^2(r)d\Omega^{(2)}. \tag{52}$$

We can interpret our black hole solution as being generated by an effective matter fluid that simulates the loop quantum gravity corrections (in analogy with the paper [51–57]). The effective gravity-matter system satisfies by definition of the Einstein equation $G = 8\pi T$, where T is the effective energy tensor. The stress energy tensor for a perfect fluid

compatible with the space-time symmetries is $T^{\mu}_{\nu} = (-\rho, P_r, P_\theta, P_\theta)$ and in terms of the Einstein tensor the components are $\rho = -G^t_t/8\pi G_N$, $P_r = G^r_r/8\pi G_N$ and $P_\theta = G^\theta_\theta/8\pi G_N$. The semiclassical metric to zeroth order in δ and a_0 is the classical Schwarzschild solution $(g^C_{\mu\nu})$ that satisfies $G^{\mu}_{\nu}(g^C) \equiv 0$.

In the following subsections we calculate the temperature, entropy and evaporation process for the semiclassical metric (34).

6.1 Temperature

In this paragraph we calculate the temperature for the quantum black hole solution and analyze the evaporation process. The Bekenstein-Hawking temperature is given in terms of the surface gravity κ by $T = \kappa/2\pi$, the surface gravity is defined by $\kappa^2 = -g^{\mu\nu}g_{\rho\sigma}\nabla_\mu\chi^\rho\nabla_\nu\chi^\sigma/2 = -g^{\mu\nu}g_{\rho\sigma}\Gamma^\rho_{\mu 0}\Gamma^\sigma_{\nu 0}/2$, where $\chi^\mu = (1,0,0,0)$ is a timelike Killing vector and $\Gamma^\mu_{\nu\rho}$ is the connection compatibles with the metric $g_{\mu\nu}$ of (51). Using the semiclassical metric we can calculate the surface gravity in $r = 2m$ obtaining and then the temperature,

$$T(m) = \frac{128\pi\sigma(\delta)\sqrt{\Omega(\delta)}\,m^3}{1024\pi^2 m^4 + a_0^2}. \tag{53}$$

The temperature (53) coincides with the Hawking temperature in the large mass limit. In Fig. 12 we have a plot of the temperature as a function of the black hole mass m. The dashed trajectory corresponds to the Hawking temperature and the continuum trajectory corresponds to the semiclassical one. There is a substantial difference for small values of the mass, in fact the semiclassical temperature tends to zero and does not diverge for $m \to 0$. The temperature is maximum for $m^* = 3^{1/4}\sqrt{a_0}/\sqrt{32\pi}$ and $T^* = 3^{3/4}\sigma(\delta)\sqrt{\Omega(\delta)}/\sqrt{32\pi a_0}$. Also this result, as for the curvature invariant, is a quantum gravity effect, in fact m^* depends only

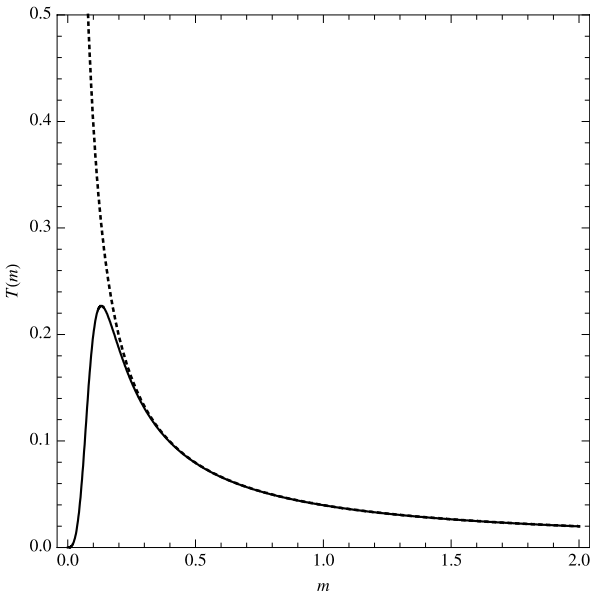

Fig. 12 Plot of the temperature $T(m)$. *The continuum plot* represent the LQBH temperature and *the dashed line* represent the Hawking temperature $T = 1/8\pi m$

on the Planck area a_0. The limit $\delta \to 0$ exists for $T(m)$ and T^*, it is:

$$\begin{aligned} \lim_{\delta\to 0} T(m) &= \frac{128\pi\, m^3}{1024\pi^2 m^4 + a_0^2}, \\ \lim_{\delta\to 0} T^* &= \frac{3^{3/4}}{4\sqrt{2\pi a_0}}. \end{aligned} \tag{54}$$

6.2 Entropy

In this section we calculate the entropy for the LQBH metric. By definition the entropy as function of the ADM energy is $S_{BH} = \int dm/T(m)$. Calculating this integral for the LQBH we find

$$S = \frac{1024\pi^2 m^4 - a_0^2}{256\pi m^2 \sigma(\delta)\sqrt{\Omega(\delta)}} + \text{const.} \tag{55}$$

We can express the entropy in terms of the event horizon area. The event horizon area (in $r = 2m$) is

$$A = \int d\phi d\theta \sin\theta p_c(r)|_{r=2m} = 16\pi m^2 + \frac{a_0^2}{64\pi m^2}. \tag{56}$$

Inverting (56) for $m = m(A)$ and introducing the result in (55) we obtain

$$S = \frac{\sqrt{A^2 - a_0^2}}{4\sigma(\delta)\sqrt{\Omega(\delta)}}. \tag{57}$$

A plot of the entropy is in Fig. 13. The first plot represents entropy as a function of the event horizon area A. The second plot in Fig. 13 represents the event horizon area as function of m. The semiclassical area has a minimum value in $A = a_0$ for $m = \sqrt{a_0/32\pi}$. As for the temperature the limit $\delta \to 0$ also exists for the entropy, we can calculate it on the event horizon area and the Planck area:

$$\lim_{\delta\to 0} S = \frac{\sqrt{A^2 - a_0^2}}{4}. \tag{58}$$

In the limit $a_0 \to 0$, $S \to A/4$.

We want underline the parameter δ does not play any regularization role in the observable quantities $T(m)$, T^*, m^* and in the evaporation process that we will study in the following section. We obtain finite quantities taking the limit $\delta \to 0$. This is an important prediction of the model.

6.3 The Evaporation Process

In this section we focus our attention on the evaporation process of the black hole mass and in particular on the energy flux from the hole. First of all, the luminosity can be estimated using the Stefan's law and it is given by $\mathcal{L}(m) = \alpha A(m) T_{BH}^4(m)$, where (for a single massless field with two degree of freedom) $\alpha = \pi^2/60$, $A(m)$ is the event horizon area and $T(m)$ is the temperature calculated in the previous section. At first order in the luminosity the metric (52) which incorporates the decreasing mass as function of the null coordinate v

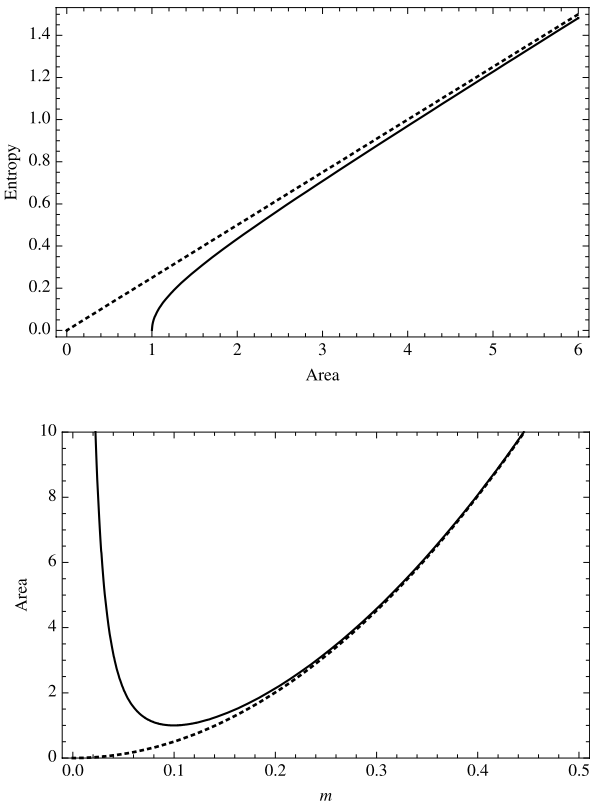

Fig. 13 *In the first plot* we have the entropy for the LQBH as function of the event horizon area (*dashed line* represents the classical area low $S_{cl} = A/4$). *In the second plot* we represent the event horizon area as function and the mass (*dashed line* represents the classical area $A_{cl} = 16\pi m^2$)

is also a solution but with a new effective stress energy tensor as underlined previously. Introducing the results (53) and (56) of the previous paragraphs in the luminosity $\mathcal{L}(m)$ we obtain

$$\mathcal{L}(m) = \frac{4194304\, m^{10}\pi^3\alpha\,\sigma^4\Omega^2}{(a_0^2 + 1024\, m^4\pi^2)^3}. \tag{59}$$

Using (59) we can solve the fist order differential equation

$$-\frac{dm(v)}{dv} = \mathcal{L}[m(v)] \tag{60}$$

to obtain the mass function $m(v)$. The result of integration with initial condition $m(v=0) = m_0$ is

$$-\frac{n_1 a_0^6 + n_2 a_0^4 m^4\pi^2 + n_3 a_0^2 m^8\pi^4 - n_4 m^{12}\pi^6}{n_5 m^9\pi^3\alpha\,\sigma(\delta)^4\Omega(\delta)^2} + \frac{n_1 a_0^6 + n_2 a_0^4 m_0^4 + \pi^2 + n_3 a_0^2 m_0^8\pi^4 - n_4 m_0^{12}\pi^6}{n_5 m_0^9\pi^3\alpha\,\sigma(\delta)^4\Omega(\delta)^2} = -v \tag{61}$$

where $n_1 = 5$, $n_2 = 27648$, $n_3 = 141557760$, $n_4 = 16106127360$, $n_5 = 188743680$. From the solution (61) we see the mass evaporate in an infinite time. Also in (61) we can take the

limit $\delta \to 0$ obtaining a regular quantity. In the limit $m \to 0$ (61) becomes

$$\frac{n_1 a_0^6}{n_5 \pi^3 \alpha\, \sigma(\delta)^4 \Omega(\delta)^2 m^9} = v. \tag{62}$$

We can take the limit $\delta \to 0$ obtaining $n_1 a_0^6 / n_5 \pi^3 \alpha\, m^9 = v$. Inverting this equation for small m we obtain: $m = [n_1 a_0^6/(n_5 \pi^3 \alpha\, v)]^{1/9}$.

7 The Metric for $\delta \to 0$

We have shown in the previous section that some physical observables can be defined independently from the polymeric parameter δ. This result entices us to calculate the limit of the semiclassical metric (34) for $\delta \to 0$. We will obtain a regular metric and we will study its space-time structure. In the quantum theory we can not take the limit $\delta \to 0$ because we do not have weak continuity in the polymeric parameter δ. However the LQBH'metric (34) is very close to the Reissner-Nordström metric which is not stable and this also suggests that (34) could also be unstable when we consider non homogeneities [58]. If this is the case then the horizon r_- could disappears from the metric, or in other words by (22), $\mathcal{P}(\delta) \to 0$. Another motivation to calculate and to study this extreme limit of the metric is to show that the polymeric parameter is not the essential ingredient in solving the singularity problem. The key ingredient is the bounce of the S^2 sphere on a minimum area. For $\delta \to 0$ the $(|p_b|/p_b^0, \log(p_c))$ plot is given in Fig. 14. We redefine the metric of section (34) introducing an explicit dependence on δ (the redefinition is: $g_{\mu\nu}(r) \to g_{\mu\nu}(r;\delta)$). The new metric is mathematically defined by

$$\lim_{\delta \to 0} g_{\mu\nu}(r;\delta) \equiv g_{\mu\nu}(r). \tag{63}$$

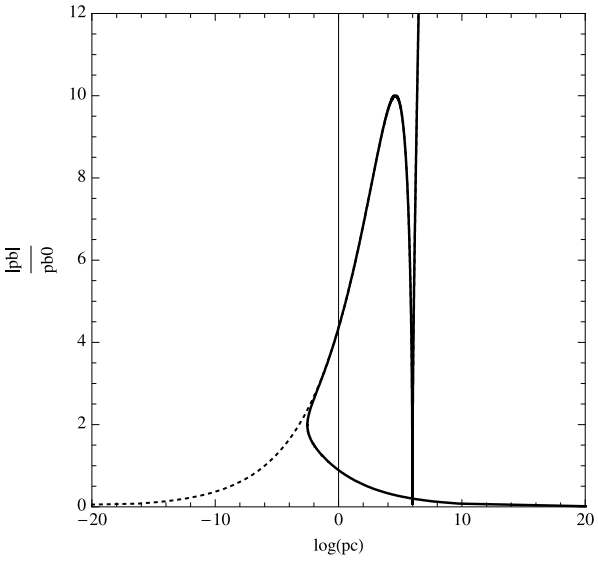

Fig. 14 Plot $(|p_b|/p_b^0, \log(p_c))$ for $\delta \to 0$. *The dashed line* represents the classical solution

The result of this limit gives the following very simple and regular metric,

$$ds^2 = -\frac{64\pi^2 r^3(r-2m)}{64\pi^2 r^4 + a_0^2}dt^2 + \frac{dr^2}{\frac{64\pi^2 r^3(r-2m)}{64\pi^2 r^4+a_0^2}} + \left(\frac{a_0^2}{64\pi^2 r^2} + r^2\right)d\Omega^{(2)}. \tag{64}$$

This metric has an event horizon in $r_+ = 2m$ and this is in accord with the solution for general values of δ, in fact $\lim_{\delta\to 0} r_- = 0$. The question now is to see if the solution is regular in all space-time and in particular in $r = 0$. We can calculate the Kretschmann invariant and we obtain

$$\begin{aligned} K(r) = {} & \frac{65536\pi^4 r^2}{(a_0^2 + 64\pi^2 r^4)^6}(-6291456 a_0^2 \pi^6 m(2m-r)r^{12} + 50331648 m^2\pi^8 r^{16} \\ & + a_0^8(15m^2 - 24mr + 11r^2) - 128 a_0^6 \pi^2 r^4(36m^2 - 56mr + 17r^2) \\ & + 4096 a_0^4 \pi^4 r^8(294m^2 - 272mr + 63r^2)). \end{aligned} \tag{65}$$

The invariant (65) is regular in all space-time and in particular at $r = 0$. For $a_0 \to 0$ we find $K(r) = 48m^2/r^6 + O(a_0^2)$ and for $r \to 0$ we have $K(r) = (983040 m^2\pi^4 r^2)/a_0^4 + O(r^3)$ that shows the non perturbative character of the singularity resolution. From the second picture in Fig. 17 is evident the r-coordinate of the peak of the curvature invariant K is independent from of black hole mass. What about temperature, entropy and the evaporation process? We calculate the surface gravity for the metric (64) and we obtain

$$\kappa^2 = \frac{65536 m^6\pi^4}{(a_0^2 + 1024 m^4\pi^2)^2}. \tag{66}$$

This result is exactly the same quantity obtained in Sect. 6 but with $\delta \to 0$. From this point the analysis is the same of Sect. 6: temperature, entropy and evaporation are identical to (54), (58), (61).

Causal Structure and Carter-Penrose Diagrams

In this section we construct the Carter-Penrose diagrams for the metric obtained taking the limit $\delta \to 0$. To obtain the diagrams we must do many coordinate changes and we enumerate them from one to five.

(1) First of all we calculate the tortoise coordinate r^* for the metric (64) defined by $dr^{*2} = -g_{11}(r)dr^2/g_{00}(r)$,

$$r^* = \frac{1}{64\pi^2}\left(\frac{a_0^2}{4mr^2} + \frac{a_0^2}{4m^2 r} + 64\pi^2 r - \frac{a_0^2 \log|r|}{8m^3} + \frac{(a_0^2 + 1024 m^4\pi^2)\log|r-2m|}{8m^3}\right). \tag{67}$$

The coordinate (67) reduces to the Schwarzschild tortoise coordinate $r^* = r + 2m\log|r - 2m|$ for $a_0 \to 0$. On the other side for $r \to 0$, $r^* \to a_0/4mr^2$. Using coordinate (t, r^*, θ, ϕ) the metric is

$$ds^2 = g_{00}(r(r^*))(dt^2 - dr^{*2}) + g_{\theta\theta}(r(r^*))d\Omega^{(2)}, \tag{68}$$

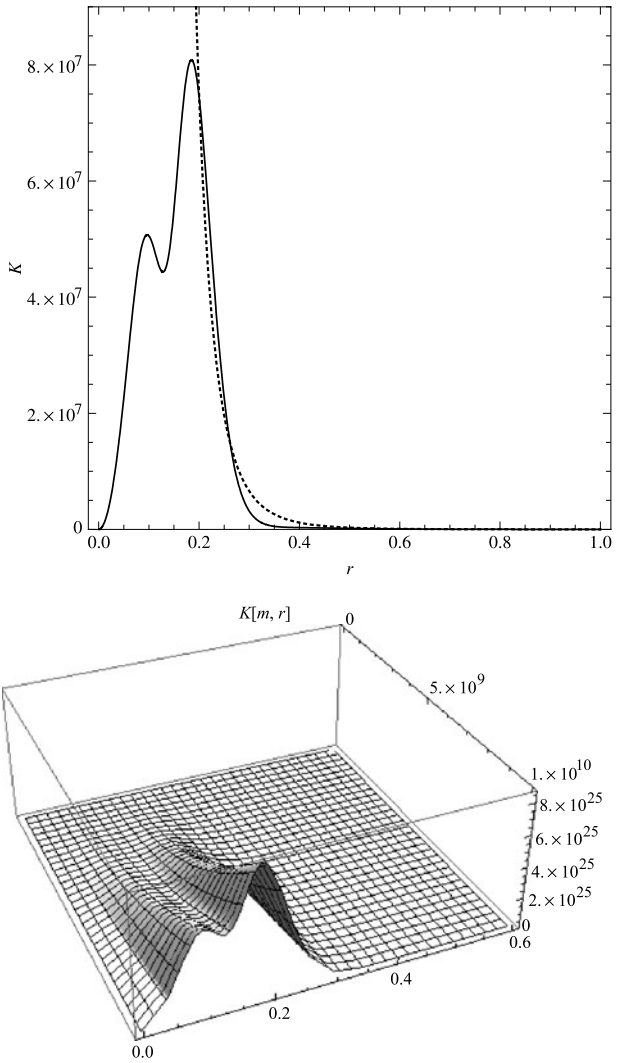

Fig. 15 Plot of the Kretschmann invariant for the metric (64). *The first picture* represent $K(r)$ and *the second* one $K(r,m)$ for $m \in [0, 10^{10}]$ and $r \in [0, 0.6]$. It is manifest the position of the maximum of $K(m,r)$ is independent of the mass m

where $g_{00}(r(r^*))$ is implicitly define by (67) (from now on we will not write the S^2 sphere part of the metric).

(2) Now we write the metric in the (v, w, θ, ϕ) coordinates defined by $v = t + r^*$ and $w = t - r^*$. The metric becomes

$$ds^2 = g_{00}(r(r^*))dvdw = -\frac{64\pi^2 r^3(r-2m)}{64\pi^2 r^4 + a_0^2}dvdw, \tag{69}$$

where r is defined implicitly in terms of v, w.

(3) We can do another coordinate changes which leaves the two-space conformally invariant. The new coordinates (v', w', θ, ϕ) are defined by $v' = v'(v)$ and $w' = w'(w)$. The metric is then

$$ds^2 = -\frac{64\pi^2 r^3(r-2m)}{64\pi^2 r^4 + a_0^2}\frac{dv}{dv'}\frac{dw}{dw'}dv'dw'. \tag{70}$$

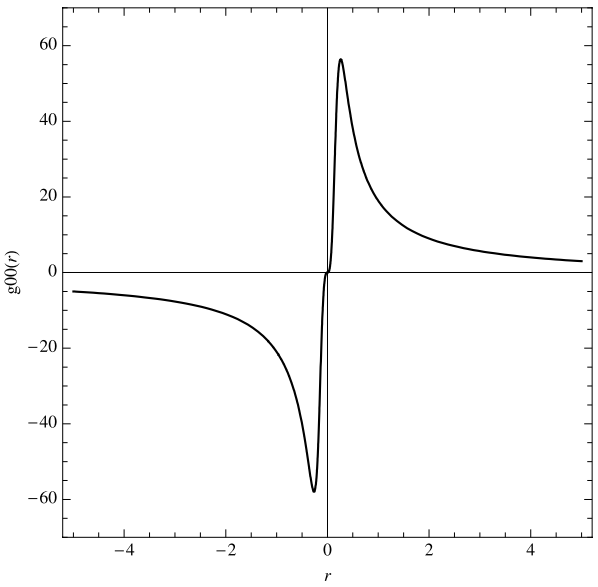

Fig. 16 Plot of $g_{tt}(r)$ for $-\infty < r < +\infty$. In the picture is not visible the horizon in $r = 2m$

(4) We introduce the new coordinates (t', x', θ, ϕ) defined by $t' = (v' + w')/2$ and $x' = (v' - w')/2$. The metric is

$$ds^2 = \frac{64\pi^2 r^3 (r-2m)}{64\pi^2 r^4 + a_0^2} \frac{dv}{dv'} \frac{dw}{dw'} (-dt'^2 + dx'^2). \tag{71}$$

All the coordinates in the conformal factor are implicitly defined in terms of t', x'.

At this point we choose explicitly the functions $v'(v)$ and $w'(w)$ to eliminate the singularity in $r = 2m$. Following the analysis of the Schwarzschild case we take $v'(v) = \exp(v/\lambda)$ and $w'(w) = -\exp(-w/\lambda)$, where $2/\lambda = 512\pi^2 m^3/(a_0^2 + 1024\pi^2 m^4)$. This is also the correct coordinate changes in our case to eliminate the coordinate singularity at the event horizon. We define the function $F^2(r) = -g_{00}(\partial v/\partial v')(\partial w/\partial w')$ that in terms of the radial coordinate r becomes

$$\begin{aligned} F^2(r) &= -\lambda^2 g_{00}(r) \mathrm{e}^{-\frac{(v-w)}{\lambda}} = -\lambda^2 g_{00}(r) \mathrm{e}^{-\frac{2r^*}{\lambda}} \\ &= 4\left(\frac{a_0^2 + 1024\pi^2 m^4}{512\pi^2 m^3}\right)^2 \left(\frac{64\pi^2 r^3}{64\pi^2 r^4 + a_0^2}\right) \\ &\quad \times \mathrm{e}^{-\frac{2}{\lambda}\left[\frac{a_0^2}{256\pi^2 mr}\left(\frac{1}{r} + \frac{1}{m}\right) + r - \frac{a_0^2}{512\pi^2 m^3} \log(r)\right]}. \end{aligned} \tag{72}$$

The metric $ds^2 = F^2(r)(-dt'^2 + dx'^2)$ is regular on the event horizon. In the coordinates (t', x') the event horizon and the point $r = 0$ are localized respectively in

$$\begin{aligned} &t'^2 - x'^2 = 0, \\ &t'^2 - x'^2 \to +\infty. \end{aligned} \tag{73}$$

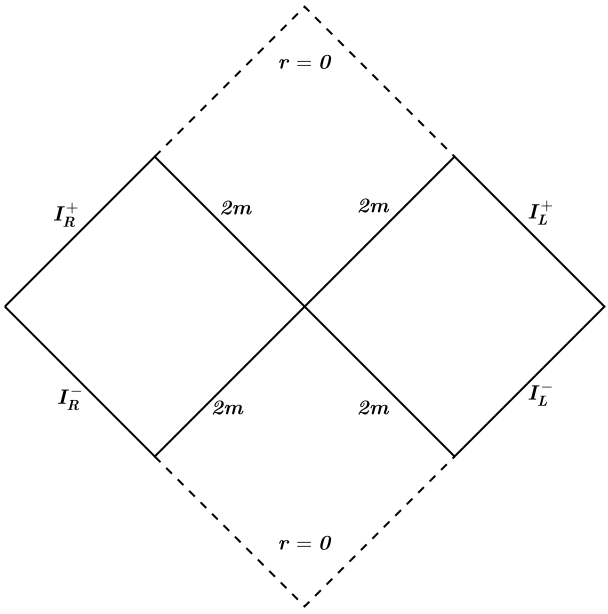

Fig. 17 Carter-Penrose diagram for the regular space-time described by the metric (64) in coordinate (ψ, ξ), the vertical and horizontal axes are respectively ψ and ξ

(5) We conclude writing the metric in the $(\psi, \xi, \theta, \phi)$ coordinates defined by $v' \propto \tan[(\psi + \xi)/2]$ and $w' \propto \tan[(\psi - \xi)/2]$. The event horizon $r = 2m$ is defined by the curve $t'^2 - x'^2 = v'w' = 0$ and then by $\psi = \pm\xi$. From (73) the point $r = 0$ is defined by the curve $t'^2 - x'^2 = v'w' = +\infty$ or by the segments $(\psi = \mp\xi \pm \pi,\ 0 \le \xi \le \pi/2)$, $(\psi = \pm\xi \pm \pi,\ 0 \le \xi \le \pi/2)$. The other sectors are: I^+, I^- $(\psi = -\mp\xi \pm \pi,\ -\pi \le \xi \le \pi)$, i^0 $(\psi = 0, \xi = \pi)$, i^+, i^- $(\psi = \pm\pi/2, \xi = \pi/2)$. The Carter-Penrose diagram of the regular space-time is represented in Fig. 17. The maximal space-time extension is represented in Fig. 18, the diagram can be infinitely extended in the two directions.

We now show that a massive particle arrives in $r = 0$ in a finite proper time. The radial geodesic equation is $(dr/d\tau)^2 = E_n^2 - 1/g_{rr}$ (τ is the proper time, E_n the particle energy) and for $r \to 0$ this reduces to $\dot{r}(1 - 64\pi^2 m r^3/a_0^2 E_n^2) = -E_n$. The $\tau(r)$ solution is $r - r_0 - 16\pi^2 m(r^4 - r_0^4)/E_n^2 a_0^2 = -E_n\tau$ and the proper time to fall in $r = 0$ starting from $r_0 \gtrsim 0$ is: $\Delta\tau = \tau(0) - \tau(r_0) = (1 - 16\pi^2 m r_0^3/E_n^2 a_0^2) r_0/E_n$. Any massive particle falls in $r = 0$ in a finite proper-time interval.

To conclude the analysis we extend the radial coordinate to negative values. The surface $\Sigma(r, \theta) = r = 0$ is a null surface as can be shown following the analysis in Sect. 3 (in particular $g^{rr}|_{r=0} = 0$). We can extend the radial coordinate r to negative values because the space-time is singularity free. The metric is asymptotically flat for $r \to -\infty$ and at the order $O(r^{-2})$ takes the form

$$ds^2 = -\left(1 - \frac{2m}{r}\right)dt^2 + \frac{dr^2}{1 - \frac{2m}{r}} + r^2 d\Omega^{(2)}, \quad r \le 0. \tag{74}$$

Because $r \le 0$ we do not have an event horizon in the negative region. The metric (64) is regular in all space-time $-\infty < r < +\infty$. The Carter-Penrose diagrams are in Fig. 19.

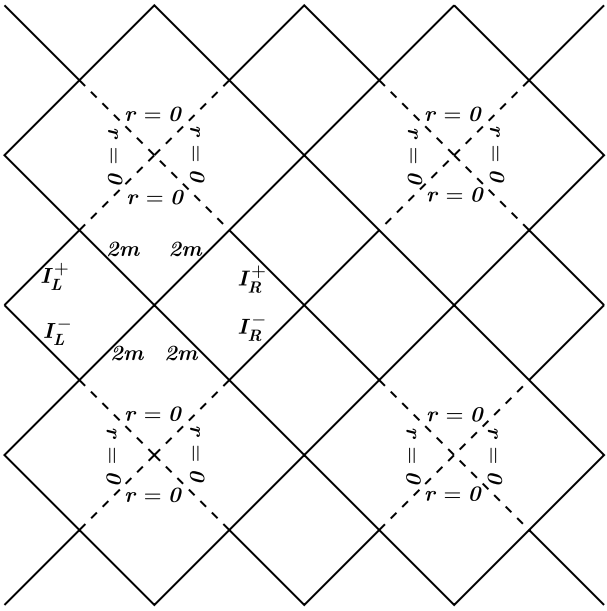

Fig. 18 A possible maximal space-time extension of the Carter-Penrose diagram in Fig. 17. In this picture we have glued four diagrams, two are placed in vertical and two in horizontal position. The point in the center represents i^0 for all the diagrams but with a different orientation

We can obtain the same results of this section in another equivalent way. Essentially what we have done in this section is to show that to solve the black hole singularity problem at semiclassical level it is sufficient to replace the component $c(t)$ with the holonomy $h = \exp(\delta c)$ without to replace the component $b(t)$ with the relative holonomy. In fact the solution (64) can be obtained directly from the *semi-quantum* Hamiltonian constraint

$$\mathcal{C}_{sq} = -\frac{1}{2\gamma G_N}\Big\{\underbrace{2(\sin\delta c/\delta)\ p_c}_{\textit{Quantum Sector}} + \underbrace{(b^2+\gamma^2)p_b/b}_{\textit{Classical Sector}}\Big\}. \tag{75}$$

The constraint (75) is an effective Hamiltonian constraint which is classic in the b, p_b sector but effective in the c, p_c sector ($N = \gamma\sqrt{|p_c|}\mathrm{sgn}(p_c)/b$ and $\sigma(\delta) = 1$). The constraint introduced in (17) is not the more general. We can introduce two different polymeric parameter δ_b and δ_c respectively in the directions θ, ϕ and r obtain the constraint

$$\begin{aligned}\mathcal{C}_{\delta_b,\delta_c} = -\frac{N}{2G_N\gamma^2}\Bigg\{&2\frac{\sin\delta_c c}{\delta_c}\ \frac{\sin(\sigma(\delta_b)\delta_b b)}{\delta_b}\sqrt{|p_c|}\\ &+\left(\frac{\sin^2(\sigma(\delta_b)\delta_b b)}{\delta_b^2}+\gamma^2\right)\frac{p_b\ \mathrm{sgn}(p_c)}{\sqrt{|p_c|}}\Bigg\},\end{aligned} \tag{76}$$

and $N = \gamma\sqrt{|p_c|}\mathrm{sgn}(p_c)\delta_b/\sin(\sigma(\delta_b)\delta_b b)$. The scalar constraint (75) is obtained taking the limit

$$\lim_{\delta_b\to 0}\mathcal{C}_{(\delta_b,\delta_c)}|_{\delta_c=\delta} = \mathcal{C}_{sq}. \tag{77}$$

The main result is that the singularity problem is solved by a bounce of the two sphere on a minimal area a_0. In this case the parameter δ does not play any role in the singularity problem resolution. It is evident from the Kretschmann invariant (65) which is independent

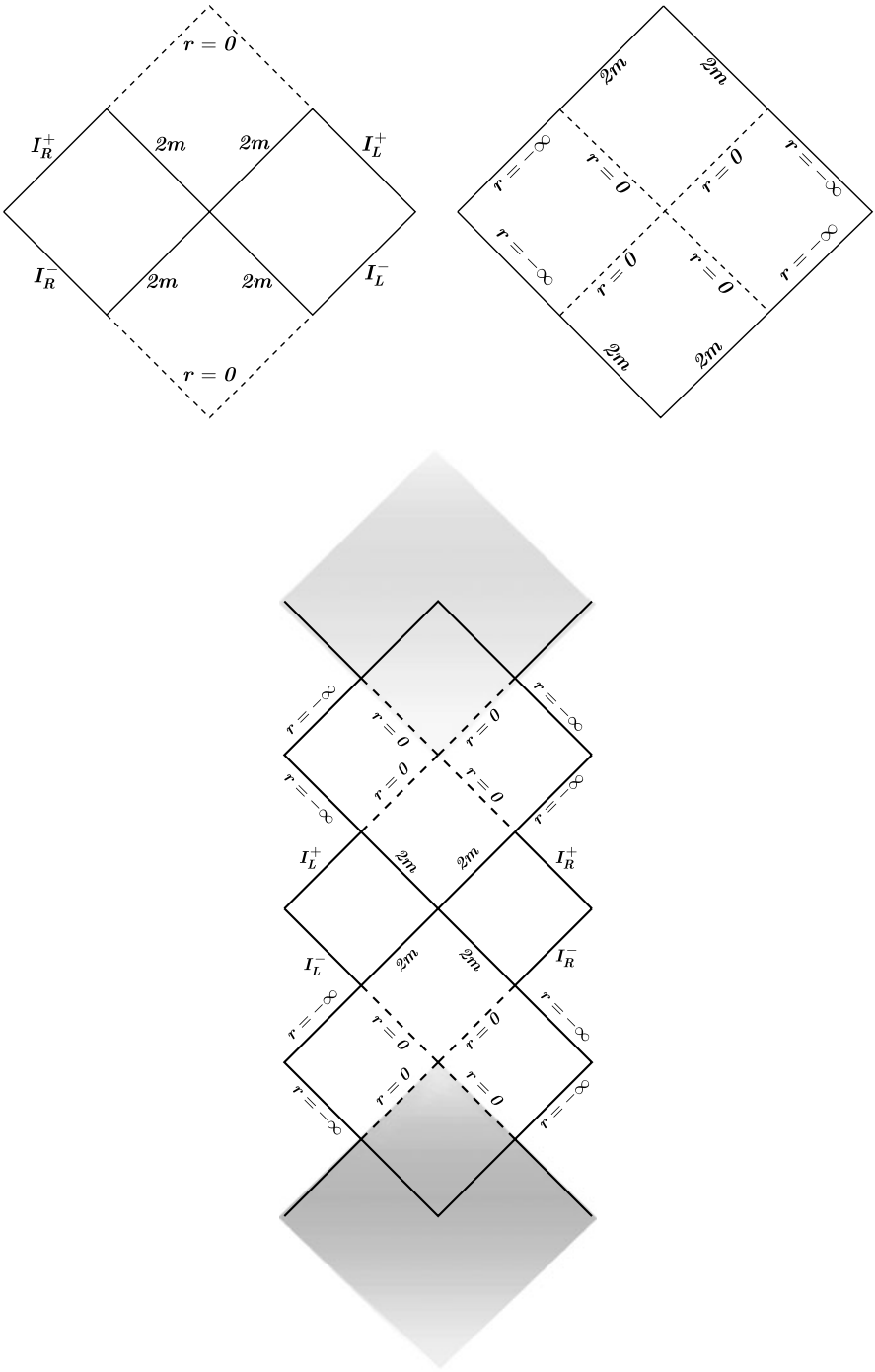

Fig. 19 Carter-Penrose diagrams for $r \geq 0$ *on the left* and $r \leq 2m$ *on the right*. *The lower picture* represents a maximal extension for $-\infty \leq r \leq +\infty$ when the two diagrams in *the upper part* of the picture are identified in the *sheared region* $0 \leq r \leq 2m$

of δ. The parameter δ is related to the position of the inner horizon and for $\delta \to 0$ the horizon r_- disappears.

8 Conclusions and Discussion

In this paper we have introduced a simple modification of the Hamiltonian constraint expressed in terms of holonomies which gives the metric with the correct semiclassical asymptotic flat limit when the Hamilton equations of motion are solved. We recall that the LQBH metric is

$$\begin{aligned} ds^2 = &-\frac{64\pi^2(r-r_+)(r-r_-)(r+r_+\mathcal{P}(\delta))^2}{64\pi^2 r^4+a_0^2}dt^2 \\ &+\frac{dr^2}{\frac{64\pi^2(r-r_+)(r-r_-)r^4}{(r+r_+\mathcal{P}(\delta))^2(64\pi^2r^4+a_0^2)}} \\ &+\left(\frac{a_0^2}{64\pi^2r^2}+r^2\right)(\sin^2\theta d\phi^2+d\theta^2). \end{aligned} \tag{78}$$

We have shown that the LQBH metric (78) has the following properties

1. $\lim_{r\to+\infty} g_{\mu\nu}(r)=\eta_{\mu\nu}$,
2. $\lim_{r\to 0} g_{\mu\nu}(r)=\eta_{\mu\nu}$,
3. $\lim_{m,a_0\to 0} g_{\mu\nu}(r)=\eta_{\mu\nu}$,
4. $K(g)<\infty\ \forall r$,
5. $r_{\mathrm{Max}}(K(g))\propto\sqrt{a_0}$.

In particular (see point 5) *the position* (r_{Max}) *where the Kretschmann invariant operator is maximum is independent of the black hole mass and of the polymeric parameter* δ. The metric has two event horizons that we have defined r_+ and r_-; r_+ is the Schwarzschild event horizon and r_- is an inside horizon. The solution has many similarities with the Reissner-Nordström metric but without curvature singularities. In particular the region $r=0$ corresponds to another asymptotically flat region. A massive particle can not arrive in this region in a finite proper time. A careful analysis shows the metric has a *Schwarzschild core* for $r\to 0$ of mass $M\propto a_0/m$.

We have calculated the limit $g_{\mu\nu}(\delta\to 0;r)$ of the LQBH metric obtaining another metric regular in $r=0$. This solution can be also obtained from (78) taking the limit $\delta\to 0$ or more simply $\mathcal{P}(\delta)=0$ and $r_-=0$. The result is

$$\begin{aligned} ds^2 = &-\frac{64\pi^2r^3(r-2m)}{64\pi^2r^4+a_0^2}dt^2+\frac{dr^2}{\frac{64\pi^2r^3(r-2m)}{64\pi^2r^4+a_0^2}} \\ &+\left(\frac{a_0^2}{64\pi^2r^2}+r^2\right)(\sin^2\theta d\phi^2+d\theta^2). \end{aligned} \tag{79}$$

This metric could be see as a solution of the Hamilton equation of motion for the *semi-quantum* scalar constraint (75).

Our analysis shows that the singularity problem is solved by a bounce of the S^2 sphere on a minimum area $a_0>0$. This happens for both the metrics obtained in this paper, the first

one of the Reissner-Nordström type (78) and the second one of the Schwarzschild type (79). *The polymeric parameter δ is not the key ingredient in the singularity resolution*. The solution (79) has all the good properties of (78) and in particular it is singularity free. This metric has an event horizon in $r = 2m$ and the thermodynamics are exactly the same as (78). When we consider the maximal extension to $r < 0$ we find a second internal event horizon in $r = 0$.

We have studied the black hole thermodynamics: temperature, entropy and the evaporation process. The main results are:

1. The temperature $T(m)$ is regular for $m \to 0$ and reduces to the Bekenstein-Hawking temperature for large values of the mass Bekenstein-Hawking
$$T(m) = \frac{128\pi m^3}{1024\pi^2 m^4 + a_0^2}. \tag{80}$$
2. The black hole entropy in terms of the event horizon area and the LQG minimum area eigenvalue is
$$S = \frac{\sqrt{A^2 - a_0^2}}{4}. \tag{81}$$
3. The evaporation process needs an infinite time in our semiclassical analysis but the difference with the classical result is evident only at the Planck scale. In these extreme energy conditions it is necessary to have a complete quantum gravity analysis that can allow for a complete evaporation [50].

$T(m)$, $S(A)$ and the evaporation process equation $\mathcal{F}(m; m_0, a_0) = v$ are regular and independent on δ for $\delta \to 0$. The result of the limit are physical quantities that depend only on the Planck area and not on the polymeric parameter.

We want to conclude the discussion with a stimulating observation. In this paper we have calculated the temperature (80) that in general we can see as a relation between temperature, mass and the minimum area a_0. If we solve (80) for the minimum area we obtain the universal critical behavior $a_0 \propto (T_c - T)^{1/2}$ near the critical temperature T_c. The critical exponent $\zeta = 1/2$ is independent of the mass and from the particular choice of the Hamiltonian constraint modification. The critical temperature is the classical Hawking temperature $T_c = 1/8\pi m$ [59].

Some Open Problems In this paper we have fixed the p_b^0 parameter (which comes from the integration of the Hamilton equations of motion) introducing the minimum area a_0 (of the full theory) in the metric solution. In this way we have obtained a bounce of the S^2 sphere on the minimum area a_0. A priori it is not obvious how to obtain the same bounce at the quantum level. However, solving the quantum constraint we believe we will obtain a bounce at a minimum area $a_0 \propto G_N\hbar$. The QEE contains only dimensionless quantities, the eigenvalues τ, μ of the operators $\hat{p}_c$, $\hat{p}_b$ and the polymeric parameter δ. When we reintroduce the length dimensions in the QEE we have $\mu \equiv 2p_b/\gamma l_P^2$, $\tau \equiv p_c/\gamma l_P^2$, then in the quantum evolution l_P^2 will play the role played by a_0 in the semiclassical analysis and we will have a quantum bounce of the wave function on $a_0 \propto l_P^2$. This is manifest in the effective Wheeler-DeWitt equation obtained from the QEE in the limit $\mu \gg \delta$, $\tau \gg \delta$ [19, 20] where $a_0^2 \propto l_P^4$ appears explicitly,
$$\sqrt{p_c}\frac{\partial^2\Psi}{\partial p_b \partial p_c} + \frac{p_b}{4\sqrt{p_c}}\frac{\partial^2\Psi}{\partial p_b^2} + \frac{1}{2\sqrt{p_c}}\frac{\partial\Psi}{\partial p_b} + \frac{p_b}{4l_P^4\sqrt{p_c}}\Psi = 0. \tag{82}$$

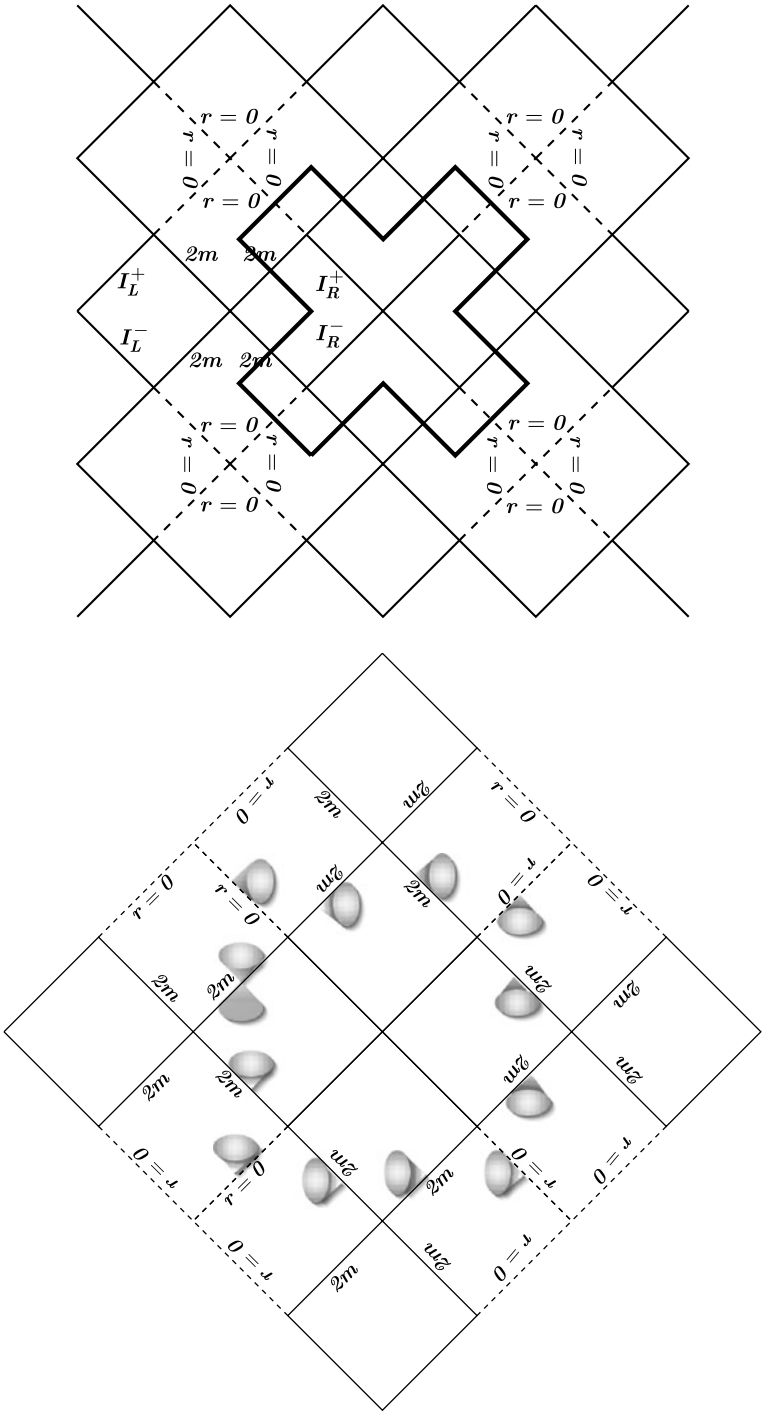

Fig. 20 Carter-Penrose diagram of Fig. 18 with evidenced a light CTC curve in *the first diagram* and the light cones along a CTC curve in *the second diagram*

However the quantum evolution of a semiclassical Schwarzschild coherent state is an open problem.

A problem related to the previous one is that we have fixed the integration in the x direction to a cell of finite volume $\mathcal{L}_x$ and this can imply a non scale invariant resolution of the singularity problem under a rescaling $\mathcal{L}_x \to \mathcal{L}'_x$ [61].

Another problem can be related to the entropy calculation. In fact we obtain a regular entropy but we do not obtain the usual logarithmic correction. We think it is possible to solve this problem with a simple modification of the Hamiltonian constraint or taking into account the possibility that quantum properties of the background space-time alter geometry near the horizon [62–67].

Other problems could be related to the maximal extension of the space-time. If we observe carefully the diagram in Fig. 18 we can see that *close time-like curve* (CTC) are possible. This is manifest in Fig. 20 where a null CTC is represented by a close black curve. In the second diagram of Fig. 20 we have represented the light cones along a CTC curve. We can have CTCs also with just one diagram if we identify the upper and lower extremes of the diagram (19).

Acknowledgements We are grateful to Parampreet Singh, Michele Arzano and Eugenio Bianchi for many important and clarifying discussions.

References

1. Rovelli, C.: Quantum Gravity. Cambridge University Press, Cambridge (2004)
2. Ashtekar, A.: Background independent quantum gravity: a status report. Class. Quantum Gravity **21**, R53 (2004). gr-qc/0404018
3. Thiemann, T.: Loop quantum gravity: an inside view. hep-th/0608210
4. Thiemann, T.: Introduction to modern canonical quantum general relativity. gr-qc/0110034
5. Thiemann, T.: Lectures on loop quantum gravity. Lect. Notes Phys. **631**, 41–135 (2003). gr-qc/0210094
6. Bojowald, M.: Loop quantum cosmology. Living Rev. Relativ. **8**, 11 (2005). gr-qc/0601085
7. Bojowald, M.: Absence of singularity in loop quantum cosmology. Phys. Rev. Lett. **86**, 5227–5230 (2001). gr-qc/0102069
8. Ashtekar, A., Bojowald, M., Lewandowski, J.: Mathematica structure of loop quantum cosmology. Adv. Theor. Math. Phys. **7**, 233–268 (2003). gr-qc/0304074
9. Ashtekar, A., Pawlowski, T., Singh, P., Vandersloot, K.: Loop quantum cosmology of $k = 1$ FRW models. Phys. Rev. D **75**, 024035 (2007). gr-qc/0612104
10. Ashtekar, A., Pawlowski, T., Singh, P.: Quantum nature of the big bang: improved dynamics. Phys. Rev. D **74**, 084003 (2006). gr-qc/0607039
11. Ashtekar, A., Pawlowski, T., Singh, P.: Quantum nature of the big bang: an analytical and numerical investigation. I. Phys. Rev. D **73**, 124038 (2006). gr-qc/0604013
12. Kantowski, R., Sachs, R.K.: J. Math. Phys. **7**(3), 433 (1966)
13. Bombelli, L., Torrence, R.J.: Perfect fluids and Ashtekar variables with application to Kantowski-Sachs models. Class. Quantum Gravity **7**, 1747–1745 (1990)
14. Modesto, L.: Disappearance of the black hole singularity in loop quantum gravity. Phys. Rev. D **70**, 124009 (2004). gr-qc/0407097
15. Modesto, L.: The Kantowski-Sachs space-time in loop quantum gravity. Int. J. Theor. Phys. **45**, 2235–2246 (2006). gr-qc/0411032
16. Modesto, L.: Loop quantum gravity and black hole singularity. In: Proceedings of 17th SIGRAV Conference, Turin, Italy, 4–7 Sep 2006. hep-th/0701239
17. Modesto, L.: Gravitational collapse in loop quantum gravity. Int. J. Theor. Phys. **47**, 357–373 (2008). gr-qc/0610074
18. Modesto, L.: Quantum gravitational collapse. gr-qc/0504043
19. Ashtekar, A., Bojowald, M.: Quantum geometry and Schwarzschild singularity. Class. Quantum Gravity **23**, 391–411 (2006). gr-qc/0509075
20. Modesto, L.: Loop quantum black hole. Class. Quantum Gravity **23**, 5587–5602 (2006). gr-qc/0509078

21. Gambini, R., Pullin, J.: Black holes in loop quantum gravity: the complete space-time. Phys. Rev. Lett. **101**, 161301 (2008). arXiv:0805.1187
22. Campiglia, M., Gambini, R., Pullin, J.: Loop quantization of spherically symmetric midi-superspaces: the interior problem. AIP Conf. Proc. **977**, 52–63 (2008). arXiv:0712.0817
23. Campiglia, M., Gambini, R., Pullin, J.: Loop quantization of spherically symmetric midi-superspaces. Class. Quantum Gravity **24**, 3649–3672 (2007). gr-qc/0703135
24. Modesto, L.: Black hole interior from loop quantum gravity. gr-qc/0611043
25. Modesto, L.: Evaporating loop quantum black hole. gr-qc/0612084
26. Bohmer, C.G., Vandersloot, K.: Loop quantum dynamics of the Schwarzschild interior. arXiv:0709.2129
27. Chiou, D.W.: Phenomenological loop quantum geometry of the Schwarzschild black hole. arXiv:0807.0665
28. Rovelli, C., Smolin, L.: Loop space representation of quantum general relativity. Nucl. Phys. B **331**, 80 (1990)
29. Rovelli, C., Smolin, L.: Discreteness of area and volume in quantum gravity. Nucl. Phys. B **442**, 593 (1995)
30. Bianchi, E.: The length operator in loop quantum gravity. Nucl. Phys. B **807**, 591–624 (2009). arXiv:0806.4710
31. Ashtekar, A.: New Hamiltonian formulation of general relativity. Phys. Rev. D **36**, 1587–1602 (1987)
32. Conrady, F., Freidel, L.: Path integral representation of spin foam models of 4d gravity. arXiv:0806.4640
33. Engle, J., Livine, E., Pereira, R., Rovelli, C.: LQG vertex with finite Immirzi parameter. Nucl. Phys. B **799**, 136–149 (2008). arXiv:0711.0146
34. Engle, J., Pereira, R., Rovelli, C.: Flipped spinfoam vertex and loop gravity. Nucl. Phys. B **798**, 251–290 (2008). arXiv:0708.1236
35. Engle, J., Pereira, R., Rovelli, C.: The loop-quantum-gravity vertex-amplitude. Phys. Rev. Lett. **99**, 161301 (2007). arXiv:0705.2388
36. Conrady, F., Freidel, L.: On the semiclassical limit of 4d spin foam models. arXiv:0809.2280
37. Alesci, E., Rovelli, C.: The complete LQG propagator I. Difficulties with the Barrett-Crane vertex. Phys. Rev. D **76**, 104012 (2007). arXiv:0708.0883
38. Speziale, S.: Background-free propagation in loop quantum gravity. arXiv:0810.1978
39. Bianchi, E., Modesto, L., Rovelli, C., Speziale, S.: Graviton propagator in loop quantum gravity. Class. Quantum Gravity **23**, 6989–7028 (2006). gr-qc/0604044
40. Modesto, L., Rovelli, C.: Particle scattering in loop quantum gravity. Phys. Rev. Lett. **95**, 191301 (2005). gr-qc/0502036
41. Bianchi, E., Modesto, L.: The perturbative Regge-calculus regime of loop quantum gravity. Nucl. Phys. B **796**, 581–621 (2008). arXiv:0709.2051
42. Bianchi, E., Satz, A.: Semiclassical regime of Regge calculus and spin foams. arXiv:0808.1107
43. Kuchar, K.V.: Geometrodynamics of Schwarzschild black hole. Phys. Rev. D **50**, 3961–3981 (1994). gr-qc/9403003
44. Thiemann, T.: Reduced models for quantum gravity. Lect. Notes Phys. **434**, 289–318 (1994). gr-qc/9910010
45. Kastrup, H.A., Thiemann, T.: Spherically symmetric gravity as a completely integrable system. Nucl. Phys. B **425**, 665–686 (1994). gr-qc/9401032
46. Thiemann, T., Kastrup, H.A.: Canonical quantization of spherically symmetric gravity in Ashtekar's selfdual representation. Nucl. Phys. B **399**, 211–258 (1993). gr-qc/9310012
47. Landau, L.D., Lifsits, E.M.: The Classical Theory of Fields. Butterworth/Heinemann, Stoneham/London (1980)
48. Ashtekar, A., Pawlowski, T., Singh, P.: Quantum nature of the big bang: an analytical and numerical investigation. I. Phys. Rev. D **73**, 124038 (2006). gr-qc/0604013
49. Fabbri, A., Navarro-Salas, J.: Modeling Black Hole Evaporation. Imperial College Press, London (2005)
50. Ashtekar, A., Bojowald, M.: Black hole evaporation: a paradigm. Class. Quantum Gravity **22**, 3349–3362 (2005). gr-qc/0504029
51. Bonanno, A., Reuter, M.: Renormalization group improved black hole space-times. Phys. Rev. D **62**, 043008 (2000). hep-th/0002196
52. Bonanno, A., Reuter, M.: Spacetime structure of an evaporating black hole in quantum gravity. Phys. Rev. D **73**, 083005 (2006). hep-th/0602159
53. Myung, Y.S., Kim, Y.W., Park, Y.-J.: Thermodynamics of regular black hole. arXiv:0708.3145
54. Myung, Y.S., Kim, Y.W., Park, Y.J.: Quantum cooling evaporation process in regular black holes. Phys. Lett. B **656**, 221–225 (2007). gr-qc/0702145
55. Nicolini, P.: Noncommutative black holes, the final appeal to quantum gravity: a review. arXiv:0807.1939

56. Banerjee, R., Majhi, B.R., Samanta, S.: Noncommutative black hole thermodynamics. Phys. Rev. D **77**, 124035 (2008). arXiv:0801.3583
57. Banerjee, R., Majhi, B.R., Modak, S.K.: Area law in noncommutative Schwarzschild black hole. arXiv:0802.2176
58. Simpson, M., Penrose, R.: Internal instability in Reissner-Nordström black hole. Int. J. Theor. Phys. **7**, 183–197 (1973)
59. Oriti, D.: Group field theory as the microscopic description of the quantum spacetime fluid: a new perspective on the continuum in quantum gravity. arXiv:0710.3276
60. Bombelli, L., Torrence, R.J.: Perfect fluids and Ashtekar variables with application to Kantowski-Sachs models. Class. Quantum Gravity **7**, 1747–1745 (1990)
61. Corichi, A., Singh, P.: Is loop quantization in cosmology unique? Phys. Rev. D **78**, 024034 (2008). arXiv:0805.0136
62. Arzano, M.: Black hole entropy, log corrections and quantum ergosphere. Phys. Lett. B **634**, 536–540 (2006). gr-qc/0512071
63. Arzano, M., Medved, A.J.M., Vagenas, E.C.: Hawking radiation as tunneling through the quantum horizon. J. High Energy Phys. **0509**, 037 (2005). hep-th/0505266
64. Banerjee, R., Majhi, B.R.: Quantum tunneling and back reaction. Phys. Lett. B **662**, 62–65 (2008). arXiv:0801.0200
65. Banerjee, R., Majhi, B.R.: Quantum tunneling beyond semiclassical approximation. J. High Energy Phys. **0806**, 095 (2008). arXiv:0805.2220
66. Banerjee, R., Majhi, B.R.: Quantum tunneling and trace anomaly. arXiv:0808.3688
67. Majhi, B.R.: Fermion tunneling beyond semiclassical approximation. arXiv:0809.1508